Wireless Personal Communications (2022) 127:1943–1983
https://doi.org/10.1007/s11277-021-08732-5

EVBlocks: A Blockchain-Based Secure Energy Trading Scheme for Electric Vehicles underlying 5G-V2X Ecosystems

Pronaya Bhattacharya[1] · Sudeep Tanwar[1] · Umesh Bodkhe[1] · Ashwani Kumar[2] · Neeraj Kumar[3,4,5]

Accepted: 29 June 2021 / Published online: 12 July 2021

Abstract

In this paper, the authors propose a secure and trusted energy trading (ET) scheme for electric vehicles (EVs) for vehicle-to-anything (V2X) ecosystems. The scheme, named as *EVBlocks*, facilitates ET among entities (i.e., EVs, charging stations (CS), and smart grids (SG)) in a secured and trusted manner through a consortium blockchain (CBC) network. The scheme operates in three phases. In the first phase, to allow real-time and resilient network orchestration of V2X nodes, we consider the ET service designed over a fifth-generation (5G) enabled software-defined networking (SDN) environment. Integration of SDN in 5G-V2X ecosystems allows V2X nodes to eliminate intermediaries and handle many requests with a minimum response time. Then, in the second phase, a non-cooperative game is presented that optimizes a cost function and converges to reach at least one Nash equilibrium point. Finally, a consensus algorithm *Proof-of-Greed (PoG)* is proposed that handles fluctuations in charging/discharging EVs through an event-driven scheduling mechanism. The obtained results are compared against parameters, such as ET time, State-of-Charge (SoC) levels, EV utility, block-convergence time, profits, computation, and communication costs. For example, *EVBlocks* achieve an average SOC charge of 22.8MW, with a peak at 377.5MW, the average power dissipation of 4.1125 kWH that is lower than 25% against existing conventional and fixed tariff schemes. The scheme converges at stable profit values for 5 EVs through a non-cooperative game. For proposed *PoG* consensus, the block convergence time for 1000 nodes is 138.96 seconds, at a computation cost of 46.92 milliseconds (ms) and communication cost of 149 bytes. The comparative analysis suggests the proposed scheme is efficient as compared to existing state-of-the-art approaches against compared parameters.

Keywords 5G · Cellular vehicle-to-anything · Electric vehicles · Energy trading · Blockchain · Non-cooperative game · Distributed consensus

✉ Sudeep Tanwar
sudeep.tanwar@nirmauni.ac.in

Extended author information available on the last page of the article

1 Introduction

Smart cities (SCs) provide sustainable growth and communication infrastructures to support the energy sector. In a similar direction, wireless communication infrastructures have transitioned from fourth generation (4G) enabled long term evolution (LTE) standards towards fifth-generation (5G) enabled communication services. 5G-enabled vehicle-to-anything (V2X) links allow short and directed relay communication in the 5.9 gigahertz (GHz) spectrum unlicensed band [27]. The band supports reliable connectivity among V2X nodes, with frequent mobility and handover access. Through 5G new radio (NR), as described in third generation partnership project (3GPP) request for comments RFC *TR 22.186*, distributed edge-based services are developed that allowed resource-based communication through flexible multicast operation support [35]. To support the latency concerns in edge-resource trading, 5G services like ultra-reliable low-latency communications (uRLLC), and enhanced mobile broadband (eMBB) are introduced that allow near response communication in V2X. Through these services, ubiquitous edge control, massive bandwidth, and dense resource profiling becomes available [4, 55]. This improves the quality of experience (QoE) for electric vehicle (EV) users in V2X ecosystems.

However, with the rise of V2X links, 5G-based uRLLC faced stringent challenges of simple network management, flexible control, and ease of programmability. To address the issue, researchers across the globe investigated the integration of software-defined networking (SDN) in 5G-V2X ecosystems to allow abstraction and decoupling of control and data plane operations [26, 49]. SDN-controlled 5G-V2X supports resilient network management, dynamic flow configurations, frequent handovers, disconnected operations, and concurrent resource interactions [22]. For EVs, integration emerged as a viable solution to handle the challenges of energy trading (ET). According to the industry forecast market survey of 2019, the global EV market is valued at $118,864.5 million in 2017 and is projected to reach $567,299.8 million by 2025, growing at a compounded annual growth rate (CAGR) of 22.3% from 2018 to 2025 [28]. This rapid rise of the global EV market requires SDN-leveraged 5G-V2X service-based solutions to meet the requirements of seamless charging infrastructures, with real-time support over operational and billing maintenance [7].

EVs support self-sustainability in 5G-V2X and performs the dual operation of transportation and energy carrier in internet-of-everything (IoE). In case of an energy deficit in IoE, EVs can purchase energy units from nearby energy nodes like charging stations (CS) or grid stations (GS), which then could be recycled back to the system in case of a deficit. However, inefficient practices may lead to mismanagement of energy demands, leading to power fluctuations. Moreover, in 5G-V2X environments, transactions are performed through centralized control planes in SDN. The central control plane is prone to network attacks like- impersonation, disclosure of private information of users, alteration of the quantity of charging units and prices, and denial-of-service to authentic users [50]. Moreover, centralized SDN control has to service bulk connection requests of clients. The transactions suffer from frequent latency issues in the case of low bandwidth channels. EVs are mainly resource-constrained nodes with limited computing and storage capabilities. This hampers the real-time interaction between CS, EVs, and associated GS in an SG. Thus, to address the aforementioned issues, a decentralized 5G-V2X edge-based mechanism is applicable to handle transactional requests and reduce computational overheads [46]. However, trading decisions need to be secured from unidentified peer malicious intruders. Such intruders could drain energy from EVs and CS by modifying energy transactional units [10]. The communication infrastructure and protocol stacks are not matured enough to handle the security issues, owing to a lack of global and open standards [43]. A comprehensive solution needs to be raised that allows EVs to query CS for energy prices in a local area, and at the same time, preserve their identity.

The issues mentioned above could be addressed by deploying a consortium blockchain (CBC) that allows only authorized stakeholders to add nodes as a chronological and timestamped ledger. This allows higher efficiency and transactional privacy than private chains and allows data provenance and consensus among EVs and CS to perform ET decisions via smart contracts in 5G-V2X ecosystems [33, 51]. Owing to limited resources, CBC needs to adopt an SDN ecosystem for network and plane management. EVs trade energy units through CS or GS via an edge-based service through SDN control planes based on measured State-of-Charge (SoC) levels to measure the energy dissipation after travelling a distance.

Through CBC, EVs trade energy with peer EVs and energy refuelling at CS, where the exchange is facilitated through a wire transfer. The billing price of energy units is added as ET and stored in CBC. Once the EVs are refilled, they can travel large distances. It is estimated that $\approx 42\%$ of energy consumption in EVs is used to propel the vehicle through a travelled distance d, and around 25% of the energy is lost in the form of heat, 23% energy of EVs is wasted to accelerate the vehicle against air drags, and 10% consumption is done in other forms [20]. Thus, EVs consistently trade energy with other IoE stakeholders and employ energy harvesting to convert mechanical energy into electrical energy stored in an EV battery. This improves the dissipation rate of SOC levels of EVs throughout the day and improves the overall mileage and covered distance of EVs. In 5G-V2X scenarios and SDN, easy decoupling achieves efficient and resilient ET services, as energy requirement messages are broadcasted in V2X networks with low latency from neighbouring roadside units (RSU) that acts as the central node to facilitate the energy transfer. The EV position is tracked through location coordinates, which are more precise and accurate in 5G-V2X based ecosystems. Once the ET is finalized, the transactions are stored in CBC and automated payments among entities are instantiated through SCs, which provides a streamlined experience to IoE users. Table 1 depicts the list of acronyms and their associated descriptions.

1.1 Motivation

Motivated from the aforementioned discussions, the paper presents an ET scheme between EVs and CS through CBC in an SDN-enabled 5G-V2X infrastructure environment. Adopting an SDN-based CBC has the dual benefits of cost-effective network management through restructuring data requests via programmable switches. Blockchain allows chronology and trust in mined transactions for authorized user groups in the 5G-V2X ecosystem. To handle resource constraints, at the SDN controller layer, we propose an edge-based service mechanism that allows task offloading that improves block creation probability and ensures better scalability of mined transactions. This addresses the challenges of an efficient charge management and SoC operational levels, which authors did not discuss in [18, 57], and [12]. Further, a dynamic pricing scheme to maximize profits of EVs and the event-driven consensus is proposed to improve the

Table 1 Acronyms and their description

Acronyms	Description	Acronyms	Description
3GPP	Third Generation Partnership Project	GS	Grid Stations
4G	Fourth Generation	IoE	Internet-of-Energy
5G	Fifth Generation	LAGs	Location Aggregators
CAGR	Compounded Annual Growth Rate	LTE	Long Term Evolution
CBC	Consortium Blockchain	NR	New Radio
CS	Charging Stations	PoG	Proof-of-Greed
CSMA	Carrier Sense Multiple Access	RFC	Request for Comments
DFS	Depth First Search	RFID	Radio Frequency Identification
ECC	Edge Computing Controller	SDN	Software-Defined Networking
eMBB	Enhanced Mobile Broadband	SG	Smart Grids
ESP	Edge Service Providers	SoC	State-of-Charge
ETaaS	Energy Trading-as-a-Service	uRLLC	Ultra-Reliable Low-Latency Communications
EV	Electric Vehicles	V2X	Vehicle-to-Anything
GPRS	General Packet Radio Service	Wi-Fi	Wireless Fidelity

response time of execution of contracts and dampen charge fluctuations. This reduces the information asymmetry and increases the lifetime of EVs rated battery capacity.

1.2 Research Contributions

The following are the main contributions of this paper.

- An SDN-leveraged edge-based environment is deployed for 5G-V2X via a CBC scheme to coordinate secure ET among EVs and CS.
- A non-cooperative game model is proposed to maximize the benefits of players and it guarantees at least one Nash equilibrium state.
- A consensus mechanism termed as *Proof-of-Greed (PoG)* is presented to minimize charge fluctuations during excess energy transfer between EVs, CSs, and GS.

1.3 Article Structure

The rest of the paper is organized as follows. Section 2 presents the related state-of-the-art schemes. Section 3 discusses the reference architecture that includes the network model, resource-trading model and problem formulation. Section 4 discusses the proposed scheme to secure ET between EVs and CSs. Section 5 discusses the performance evaluation of *EVBlocks*. Section 6 presents the limitations of BC-based ET schemes and future directions, and finally, Sect. 7 concludes the paper.

2 State-of-the-Art

The section discusses the recent state-of-the-art schemes for responsive V2X communication, resource management, allocation, and ET in V2X scenarios. Researchers worldwide are working towards the integration of 5G services in V2X environments to provide responsive and resilient solutions for resource allocations and optimize energy management. For example, Sharma *et al.* [41] studied about 5G-V2X security schemes and compared them with existing 4G-LTE services. They proposed a novel security reflex architecture for ultra-dense transmission and mobility support in 5G-V2X. Rasheed *et al.* [38] demonstrated ultra-low delay V2X transmissions based on 5G millimeter wave (mmWave) systems that can support > 1 Gbps user bandwidth. The authors proposed 3D-based position beam alignment schemes to segment the road traffic into different groups, with group authentication provided through elliptic curve cryptography. However, the security validations are not discussed in the proposed approach. Do *et al.* [15] discussed about non-orthogonal multiple access scheme for 5G-V2X infrastructures. The author's proposed vehicular communications through multiple antennas over Nakagami-m fading channels and studied outage probability and successive interference cancellation (SIC) of vehicles. They found out the outage performance of NOMA-V2X based on channel fading parameters, imperfect SIC, and NOMA-based power allocation factors through analysis. Chen *et al.* [13] discussed cellular V2X evolution with 5G-NR to leverage low-latency and high-throughput for vehicular communication. The technical evolution of the standards about NR-V2X is discussed and is compared to the 4G counterparts.

In resource trading, load balancing, and optimizing energy management for EVs, researchers across the globe have proposed efficient schemes for V2X infrastructures. For example, Hua *et al.* [21] implemented smart contracts-based solutions to manage battery refuelling and swapping to facilitate the trust management issue charging EVs and GS. The security vulnerabilities of managing and executing smart contracts are not discussed. Authors in [8, 57] designed a blockchain-based renewable energy incentive system for EVs that provides additional incentives to users. The aforementioned works failed to address issues of scalability, integrity, and user privacy.

Authors in [9, 24] presented an edge-as-a-service scheme to manage ET of EVs in an SDN scheme for vehicle-to-grid (V2G) platforms to reduce the overall latency of the system. Chaudhary et al. [12] proposed a CBC to manage SoC levels for battery refueling of EVs in the SDN environment. Hayes et al. [18] proposed a peer-to-peer trading scheme for trading energy in SG by balancing network voltage profiles. A more comprehensive analysis of user profiles and base voltage is required.

Florea et al. [16] proposed an efficient battery management system, that allows battery swap from nearby registered stations and facilitates the transaction, BC-based ledgers are proposed. For payments, two payment modes are made available. The first mode allows payments through ethereum based SC, and the second mode designs a directed acyclic graph (DAG) system, with a proposed IOTA tangle for data-driven battery management. However, the scheme does not address the privacy and security constraints of shared user data. The payment mode through the IOTA tangle allows even non-registered users to gain access to the BC network. Thus malign users can launch fake propagation updates, which poses a critical issue. Samuel et al. [40] proposed ET based on a game model that allows demand-responsive pricing and addresses the issue of demurrage payments for IoE stakeholders. However, the scheme has not considered the genuineness of added users in the proposed game, allowing malicious users to increase demand, and correspondingly, the prices hike up. Authors in [2] proposed a peer-to-peer ET scheme *UBETA*, for permissioned BC, and designs a hyper-ledger-driven consensus named as *Hyperledger Basu*, that operates on a node-size of 60 nodes. However, with increasing node additions, the obtained transactional throughput gets affected, which is not considered. Jamil et al. proposes ET to achieve optimal power and energy crowd-sourcing on a real-energy dataset collected from Jeju province of the Republic of Korea. The scheme supports ET among the consumer and prosumer and is based on real-time scheduling and control of SG loads and demands throughout the day. The collected time-series data is analyzed to form accurate predictions on the model performance, and the simulation is performed on various metrics. The performance of BC is analyzed through resource utilization, latency in node additions, and resource utilization. However, machine learning (ML) algorithms are not compared to diverse metric sets.

The presented state-of-the-art schemes have focused on ET through BC based on resource pricing, SC, predictive models, and demand-forecast pricing. Some schemes have to combine SDN with BC to effectively orchestrate the network and leverage effective management through the programmable nodes. However, none of the works has proposed a coherent presentation of ET in V2X ecosystems that combines the key benefits of SDN to facilitate edge-based ET services, dynamic pricing scheme, and consensus to achieve flexibility and management of charging and discharging profiles of EV. To address the research gap, we present the scheme, *EVBlocks*, that unifies the key concepts of BC-based secure ET with SDN-based ET services, coupled with effective models for dynamic pricing and consensus schemes to manage additional charge levels. Table 2 presents a comparative analysis of existing schemes with the proposed scheme.

3 *EVBlocks*: The Reference Architecture

The section proposes the reference architecture of *EVBlocks* based on the SDN-leveraged 5G-V2X infrastructure ecosystem. This section discusses the 5G-V2X network model, the resource-trading model, and the problem formulation of the proposed architecture.

3.1 The Network Model

The section proposes the network model of the proposed scheme. The section discusses the communication infrastructure, the components, and the reference 5G components. Figure 1 discusses the proposed network model for *EVBlocks* trading scheme based on 5G-V2X ecosystems.

3.1.1 5G-V2X Channel

In the 5G-V2X ecosystem, we consider a mmWave channel-based communication that operates on the range from 30-300 GHz range. In C-V2X, any two nodes N_1 and N_2 communicate based on transmitting and receiving antennas, denoted as A_t and A_r respectively. The aggregate channel matrix can be modelled as follows [19],

$$M(t) = \sum_{E_{cl}}^{E_t} \sum_{p}^{N_p} M_{E_{cl}} \cdot p(t) \tag{1}$$

Table 2 Comparative analysis of proposed scheme against existing state-of-the-art schemes

Research	Year	Parameters							Objective	Pros	Cons
		1	2	3	4	5	6	7			
Hua et al. [21]	2018	Y	N	Y	N	N	N	N	BC-based battery refueling for EV, and proposed ethereum based SC to facilitate payments	Proposed slots for fair charging evaluation via measurement of energy levels	The authors have not considered the feasibility of batter refueling through extensive real-world simulations
Zhang et al. [57]	2018	Y	N	Y	N	Y	Y	N	An incentive-based cryptocurrency scheme for ET among EV,	Through priority-based incentives, the proposed scheme achieves a Nash equilibrium that optimizes ET sharing	The scheme does not discuss the security trade-offs while proposing incentives of different EV through the game model.
Jindal et al. [24]	2019	Y	Y	Y	Y	N	Y	N	A BC-based ET scheme named *SURVIVOR*, where approver nodes are selected for validation of transactions in SDN environment	During ET, load profiles of EV and SG are considered before and after transactions, and via SDN edge-based ET scheme is presented	The authors have not considered the deployments in consortium BC, and have to address trading scenarios during vehicle movements, and content caches
Chaudhary et al. [12]	2019	Y	Y	Y	Y	N	Y	Y	BC-based ET scheme, *BEST*, where energy nodes are validated on basis of dynamic pricing, and connectivity records	SDN based ET to facilitate responsive edge transactions, supported through tactile internet	Flow-control policies in SDN is not discussed, that ensures mass connectivity and scalability of ET transactions
Sharma et al. [41]	2020	N	Y	N	N	N	Y	Y	A security based scheme for 5G-C-V2X	Security-reflex function (SRF) reduces burden of vehicular mobility management	Authors have not considered the issues of credential thefts and dense sensor based replay attacks
Rasheed et al. [38]	2020	N	Y	N	N	N	N	Y	3D-beam alignment scheme for C-V2X for mmWave 5G	A dynamic vehicle routing scheme is proposed based on optical beam selection , that improves the V2X performance	Security consideration are not discussed while routing data among diffferent V2X nodes
Do et al. [15]	2020	N	Y	N	N	N	N	Y	NOMA-based communication in V2X supported over Nakagami-m fading channels	Relay-assisted broadcasting supported NOMA that improves connection density, spectrum efficiency, low latency and high relaibility in V2X	Numerical simulations on antenna selection to optimize the outage performance of NOMA-V2X is not considered

Table 2 (continued)

Research	Year	Parameters							Objective	Pros	Cons
		1	2	3	4	5	6	7			
Chen et al. [13]	2020	N	Y	N	N	N	N	Y	A vision and road-map of emergence of C-V2X from LTE-V2X to NR-V2X is presented	The article discusses the technical standards and deployments of C-V2X	Channel modelling and edge based computations in C-v2X are not considered
Hayes et al. [18]	2020	Y	Y	Y	N	Y	N	N	BC-based double auction trading to facilitate peer-to-peer ET payments	Modelling of three-phase distribution networks through MATLAB Open DSS, that allows ET for local distribution networks	The sensitivity of the distribution networks and its impact on ET trading is not considered
Florea et al. [16]	2020	Y	N	Y	N	N	Y	N	BC- based battery management system (BMS)	BC-implementation for battery swap and charge to facilitate ET is addressed via Ethereum, and direct acyclic graph based IOTA	Tag-based IOTA algorithms by non-registered users, that can add fake transactions in the ecosystem
Samuel et al. [40]	2021	Y	Y	Y	N	N	Y	N	Authors propose ET scheme with demand response pricing model , with inclusion of demurrage fees	Secure ET in CBC that addresses the disputes among IoE stakeholders through demurrage payments through BC	Authors did not consider a reputation management system that might be compromised through malicious aggregators
Abdella et al. [2]	2021	Y	Y	Y	N	N	Y	N	Propose a unified peer-to-peer permissioned blockchain scheme for ET environments, and named it UBETA	Designed a scheme known as *Hyperledger Basu*, with a network size of 60 nodes and real ET data from western Australia energy market	Scalability with more nodes in the experimental setup is yet to be considered
Jamil et al. [23]	2021	Y	N	Y	N	N	Y	N	BC-based predictive ET platform with real-time energy fluctuation analysis throughout the day	Optimal power flow and energy crowd-sensing to leverage ET among consumer and prosumer	Comparative analysis of machine learning algorithms on diverse parameters set is not discussed
Proposed	2021	Y	Y	Y	Y	Y	Y	Y	CBC based ET scheme in 5G-V2X ecosystems	SDN is employed to allow ET-as-a-Service (ETaaS), and for charging profiles novel consensus is proposed	Inherently complex due to a large number of communication points with discrete states

1. Energy Trading 2. Latency 3. Trust 4. SDN 5. Game Model 6. Consensus 7. 5G/6G , Y-shows parameter is considered, N-shows parameter is not considered

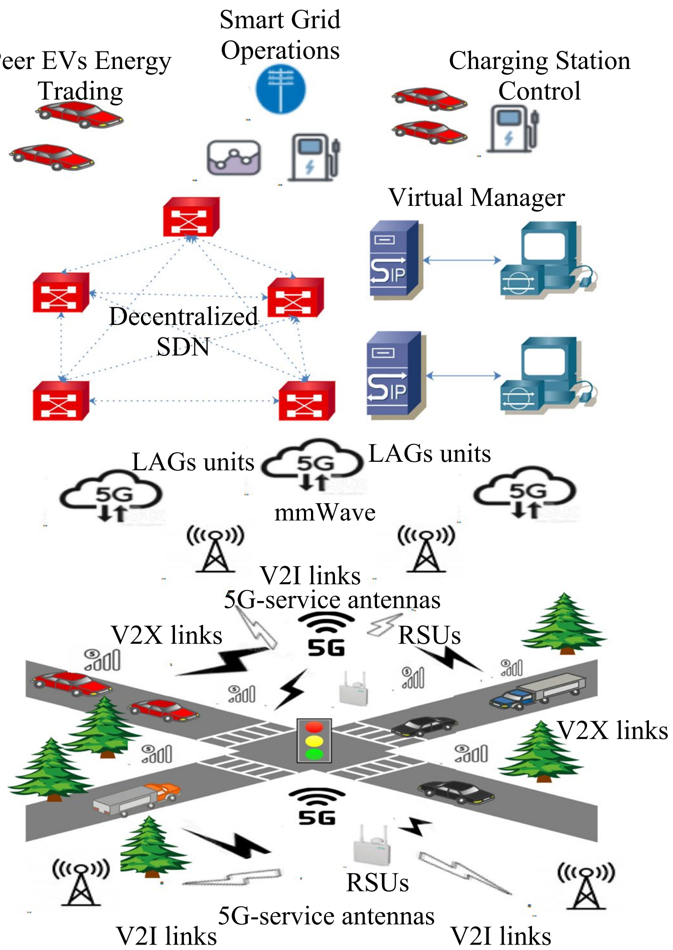

Fig. 1 *EVBlocks*: SDN-leveraged network model underlying 5G-V2X communications

where E_{cl} denotes the total EV units that communicates with RSU units, E_t is the total V2X nodes, p denotes the nodes that participates in communication, and N_p denotes the communication signals inside each communicating RSU. $M_{E_{cl}}.p(t)$ denotes the single mmWave channel contribution to any p^{th} node in N_p, at any given time instant t. The path loss model of mmWave depends on signal shadowing between A_t and A_r, over a communicating distance d, at a given carrier frequency f. The path-loss P_L in decibels (dB) is defined as follows [19],

$$P_L(dB) = (P_{L_0} + 10_{\eta_p} log(d/d_0)) + Q_{\sigma_s} \tag{2}$$

where d_0 denotes the free-space reference distance, P_{L_0} denotes the free-space loss at a given distance d_0, η_p denotes the path loss exponent, and Q_{sigma_s} denotes the normal log shadowing model. Based on Q_{sigma_s}, any k^{th} entity EV position is determined based on associated distance d_{EV_k} and predicted angle θ_{EV_k}. To notion the prediction, we consider a spatial beam-forming process deployed within a servicing RSU unit to support bi-directional communication among peer EVs. To model the same, we consider the EV set $\{EV_1, EV_2, \dots, EV_k\}$, divided into two bipartite regions, one denotes the source (S), and the other denotes the destination (D), respectively. We consider two EVs P and Q, separated through a distance d. The 5G-service antennas model the distance prediction based on 3D-spherical coordinates denoted via latitude and longitude pairs. For EV P we denote the pair as $P(\theta_1, \phi_1)$, and for EV Q, we denote the pair as $P(\theta_2, \phi_2)$. The spherical coordinates through the 5G-antenna can be depicted as follows,

$$x = rcos\theta cos\phi \tag{3}$$

$$y = rcos\theta sin\phi \tag{4}$$

$$z = rsin\theta \tag{5}$$

where (x, y, z) represents the 3D-spherical co-ordinates for EV pairs P and Q respectively, r denote the radius, θ denotes the latitude, with constraint, $(-\pi/2 \leq \theta \leq \pi/2)$, and ϕ denotes the longitude, with constraint as $(0 \leq \phi \leq 2\pi)$. The distance D_{PQ} between points P and Q can be computed based on Euclidean distance as follows.

$$D_{PQ} = \sqrt{(x_1 - x_2)^2 + (y_1 - y_2)^2 + (z_1 - z_2)^2} \tag{6}$$

Based on D_{PQ}, the EVs position can be computed. At any general co-ordinate (u, t, w), the EV predicted mobility in 5G can be derived as follows,

$$\begin{aligned} P_{PQ}(u, t, w) &= V_{pos}(u) + D_{PQ}rcos\theta cos\phi \\ &= V_{pos}(t) + D_{PQ}rcos\theta sin\phi \\ &= V_{pos}(w) + D_{PQ}rsin\theta \end{aligned} \tag{7}$$

where P_{PQ} denotes the predicted covered distance by EVs at general point (u, t, w). Based on the predicted position, the beam gain (in dB) of 5G antenna can be depicted as follows,

$$G_v = \frac{4\pi r^2}{\pi(r^2 \tan^2(\theta_{max}/2))} \tag{8}$$

where θ_{max} denotes the maximum 5G-antenna beam-width and is formulated as follows.

$$\theta_{max} = 2\tan^{-1}\sqrt{\frac{4}{G_v}} \tag{9}$$

As RSU units deploy 5G-uRLLC services, parallel beam-forming antennas can be selected based on matching SDN rule set R. The 5G channel metrics can be depicted as follows,

$$C_V = Blog_2(1 + S/N) \tag{10}$$

$$S/N = 10log_{10}(\frac{S_A}{R_A}) \tag{11}$$

where C_V denotes the 5G-channel capacity, B denotes the bandwidth, S/N denotes the signal-to-noise ratio, and S_A and R_A denotes the signal strength at the sending and receiving antennas respectively. The receiver signal power $P(R_A)$ can be determined as follows,

$$P(R_A) = S_A + G_v - Q_c \tag{12}$$

where Q_c denotes the path loss exponent of the channel.

3.1.2 SDN Integration With 5G-V2X

As depicted in Sect. 3.1.1, 5G-channel antennas compute D_{PQ} to form intelligent predictions P_{PQ} among two-point sets P and Q for EVs to allow an SDN-rule based policy framework at higher layers. To form the matching rule set R, decentralized SDN controllers are installed to perform network hypervisor services. To manage the trust among SDN nodes, a CBC approach is applicable. A local controller C_L is installed at each SDN node to communicate with the 5G-core data plane [29]. To formulate the same at data plane, a wireless manager W_M is installed that schedules resource sets based on virtual 5G-slicing $\{S_1, S_2, S \ldots, S_l\}$. Thus, multiple virtual networks are instantiated, managed through SDN-virtual resource managers based on the supply and demand of resources. These virtual managers dynamically adjust the demand-response ecosystems based on available channel capacity C_V and predicted gain G_V. The details of the resource-trading model are now presented in the following section.

3.2 Resource-Trading Model

This section comprises two subsections-SDN-leveraged CBC resource-trading model and the associated problem formulation. Resource-trading model is divided into three layers, *Layer 0*, *Layer 1*, and *Layer 2*, depicted as follows.

3.2.1 SDN-Leveraged CBC Resource-Trading Model

An SDN-based CBC architecture is proposed for 5G-V2X infrastructure, as shown in Fig. 2. The data movement is from the lower layer *Layer 0* to the higher layer *Layer 2*. *Layer 0* is the data layer that generates energy transactions among entities like EVs, CS, and GS. EVs interact for energy exchange with CS located over-communicating GS with the desired frequency range. Inside every GS, there are smaller micro-grids, termed as location aggregators (LAGs), to facilitate load-balancing of GS. This provides faster resolution to EVs during ET between EVs and CSs. LAGs can gather energy data generated by EVs and CSs in their local proximity (*intra*) or forward requests to other LAGs via GS to CS in other spatial coverage range (*inter*). LAGs forward meta-data information {bytes_exchanged, transaction_time, ID (EV), ID (CS), ID (LAG)} to *Layer 1*, thereby decreasing the volume of raw-data. *Layer 1* is the decentralized SDN controller layer used to manage the network forwarding through routers [48]. Then, it executes the 5G-virtual slicing through hypervisors to manage EV charging requests and perform computational offloading closer to the edge nodes in *Layer 0*. Instances of virtual switches are created to cater to requests. *Layer 2* is an energy transactional layer that collects the user transactional information among EVs and CSs from remote locations. Moreover, it provides a consensus

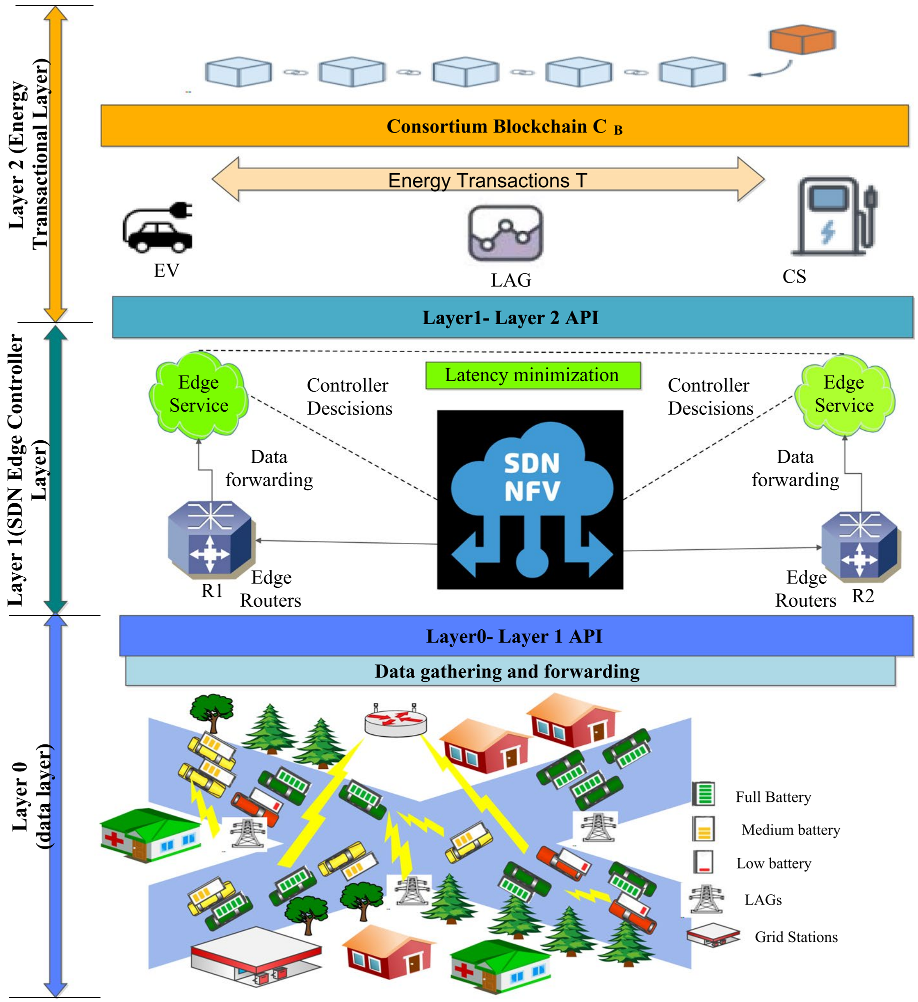

Fig. 2 *EVBlocks*: SDN-leveraged CBC resource-trading model

mechanism to record transactional data on the chain as an agreed set of truths among participating entities.

3.2.2 Problem Formulation

As depicted in subSect. 3.2.1, a CBC scheme operating over the SDN environment is proposed to secure ET between EVs and CSs over a LAG. The following is depicted in Fig. 3. To provide computational services to LAG and handle large trading requests, edge service providers (ESP) are present. The functionality of EVs, LAG and ESP are now presented as follows.

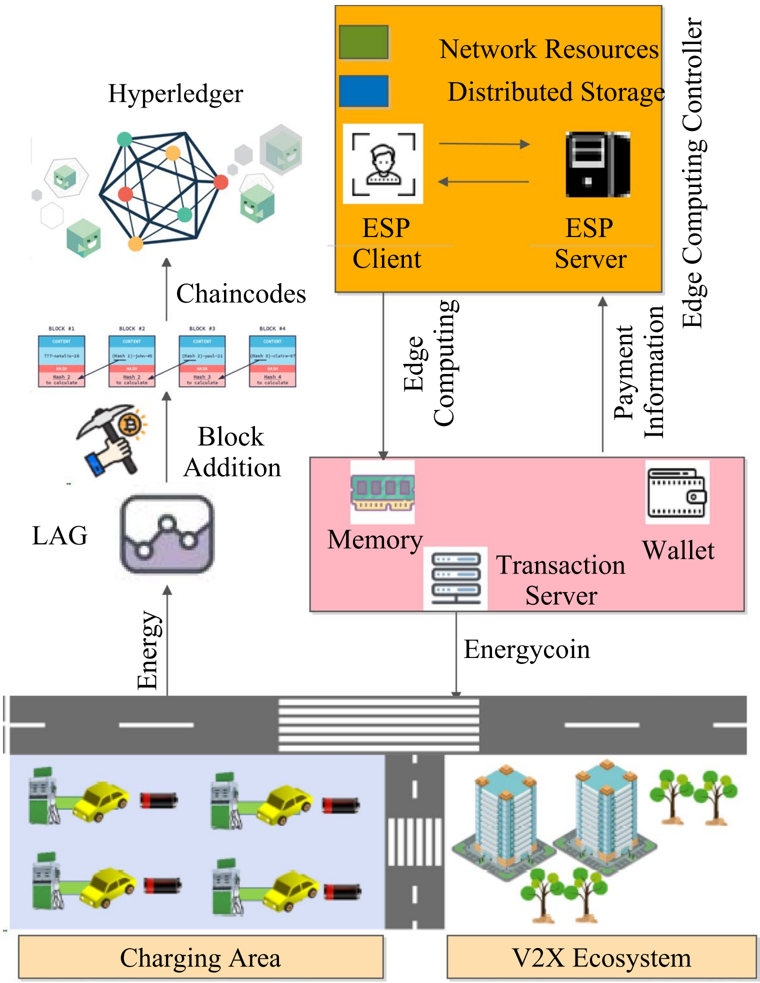

Fig. 3 CBC-based ET in 5G-V2X ecosystem

– *EVs*: In the proposed scheme, EVs and CS aggregate the data for ET at the data layer. EVs mainly acts as an energy container because they supply energy back to GS during peak hours.
– *LAG*: At SDN, LAGs provides edge computing services to EVs via edge computing controller (ECC). ECC monitors information dissemination, location updates, SoC levels, and perform energy transactions supported by green cryptocurrency *Energy-Coin* to be added to wallet *W*. LAGs require a transactional server (TS) (*T*), a memory unit (*M*), and cryptocurrency wallet (*W*) to support distributed heterogeneous requests. To ensure the privacy of EVs, the wallet (*W*) is added with a *nonce*, which generates random identifiers. *W* is mapped with corresponding *T* to ensure payments to correct recipients.
– *Edge service providers*: ESPs integrate the computations and network resources to provide a unified set of services based on a client-server model. It leverages edge computing services for LAGs [9]. The ESP issues a price for its service, and each LAG

determines the service demand be purchased based on the price. Then, computation-intensive mining can be offloaded from a LAG to its proximate edge computing nodes instead of being processed locally or by remote cloud nodes.

The layer-wise description of the entities, as depicted in 3.2.1 are as follows.

- **Layer 0**: Consider a set of communicating GS $G = \{G_1, G_2, G_3, \dots G_n\}$ with coverage range as $\{r_1, r_2, \dots, r_n\}$. Each range r_i has LAGs $L = \{L_1, L_2, \dots, L_n\}$. Any i^{th} LAG L_i facilitates as vehicular aggregator for ET with a total of p EVs, denoted as v_p within L_i. Out of p vehicles, consider a k^{th} instance of v_p to denote any selected k^{th} vehicle in an i^{th} LAG, as V_k^i, such that $1 \leq i \leq n$, and $1 \leq k \leq p$, respectively. Generated data from v_p is collected and sent to SDN controller through virtual SDN switches associated with it at *Layer 1*.
- **Layer 1**: As part of SDN controller layer, consider any k^{th} EV data instance selected from v_p, an utility function U_k^i is defined to optimally select k^{th} node in the i^{th} LAG as follows,

$$U_k^i = (U_i^{th} \times B_k^i)/(p \times B_k^i) \times D_{k \leftarrow i/r} \tag{13}$$

where U_i^{th} is the maximum utilization factor of the SDN virtual switch, B_k^i is the ideal bandwidth of the k^{th} node in the i^{th} LAG, and $D_{k \leftarrow i/r}$ is the average latency for the distance travelled by k^{th} EV to the i^{th} LAG to charge where the computational processing takes place at the r^{th} node of the system.
- **Layer 2**: At energy transactional layer, consider k^{th} EV, and c^{th} CS, respectively, in the i^{th} LAG, denoted by V_k^i and V_c^i. k^{th} EV and c^{th} CS want to trade energy over a CBC network C_B having w nodes. To facilitate the trading scenario, k^{th} EV performs a wallet transaction T_i with c^{th} CS as follows,

$$T_i = \{I_{k \rightarrow c}^i, D_{k \rightarrow c}^i, nonce, C_{k \rightarrow c}^i\} \tag{14}$$

where $I_{k \rightarrow c}^i$ is information (control) units with scheduling, routing, and location information shared by k^{th} EV to c^{th} CS under the supervision of the i^{th} LAG. $I_{k \rightarrow c}^i$ is shared prior to payload bursts, denoted as $D_{k \rightarrow c}^i$ by k^{th} EV to c^{th} CS in the i^{th} LAG, and *nonce* is a unique pseudo-random number that includes timestamp information, and $C_{k \rightarrow c}^i$ is the credits distribution by k^{th} EV in i^{th} LAG. Similarly, the transactions super-set T will contain sub-transactions of all LAGs.

$$T = \{T_1, T_2, \dots, T_n\} \tag{15}$$

The information over the blockchain network C_B is rewarded as follows.

$$C_B = \{H_{prev}, nonce, T_i, Merkle\_root\} \tag{16}$$

The transactions performed over the blockchain C_B can be secured for discharging total energy of v_p EV units. In v_p, the discharging information for EVs is denoted as $D[EVs] = \{D_1, D_2, D_3, \dots D_i\}$. Session data is secured by generating pseudo-random sequences of numbers $\{\rho_1, \rho_2, \dots, \rho_i\}$ for v_p to gain access as a challenge from L_i and launch a session in C_B. Then, the session data is set to the closest grid stations G_k through a c^{th} LAG L_c. Then, the shared data of transaction follows the pattern for symmetric encryption as follows.

$$E_{LG}[k, [C_B||G_k||L_c||\rho_i^n||Merkle\_Root]] \tag{17}$$

For asymmetric encryption, we first hash the C_B information with LAG hash value H_{LAG} and form a combined hash H' as follows.

$$H' = H_{LAG}||C_B \tag{18}$$

Then, H' is encrypted using the public key of grid G, denoted by Pub(G), which is represented as follows.

$$E[Pub(G), [C_B||G_k||L_c||\rho_i^n||Merkle\_Root]] \tag{19}$$

The corresponding grid decrypts the CS transaction using its private key $P_r(G)$ as follows.

$$D[P_r(G), [E[Pub(G), C_B||G_k||L_c||\rho_i^n||Merkle\_Root]] \tag{20}$$

Based on public/private key pairs of GS, a secure ET is proposed in C_B between EVs and CSs over a LAG. Now, any k^{th} EV in i^{th} LAG that wants to trade energy with c^{th} CS, sends its credentials as follows,

$$C_k = \{ID_{EV}^k, P_{eu}, nonce\} \tag{21}$$

where C_k is the credential information of k^{th} EV, P_{eu} is the energy price unit cost, and *nonce* is timestamp identifier. The following computations are handled by a j^{th} edge node at SDN controller layer that computes the hash of the transaction as follows,

$$H[C_k] = SHA - 256(C_k, Cert(j), J_i^k) \tag{22}$$

where a 256 bit fixed output is formed using identity of j^{th} node, and J_i^k is the desired SOC level of the battery, i.e., the rated capacity. The energy accumulated by the j^{th} edge node in the i^{th} LAG, is required by k^{th} EV to perform energy transaction with c^{th} CS as follows,

$$J_i^{req} = (L_{i_{SOC}}^{max} - L_{i_{SOC}}^{r}) \times J_i^k \tag{23}$$

where $L_{i_{SOC}}^{max}$ is the maximum SOC that can be attained and $L_{i_{SOC}}^{r}$ is the rated EV capacity. A threshold Th_{min} is set for each EV to trade energy with c^{th} CS. Thus, the available average energy J_i^{av} is computed as follows.

$$J_i^{av} = (J_i^{req} + Th_{min})/p \tag{24}$$

The energy dissipation loss L_{dis}^k for k^{th} EV is calculated as follows,

$$L_{dis}^k = \int_0^{J_i^r} [(J_i^{av} - J_i^{curr})(L_{i_SOC}^{max} - L_{i_SOC}^{req})] \tag{25}$$

where L_{dis}^k denotes energy dissipation for k^{th} EV in transit. Since EVs have limited computing resources, it is critical to compute energy loss of any k^{th} EV at time instant t. J_i^{curr} denotes the current SOC charge levels in i^{th} LAG and $L_{i_SOC}^{req}$ is the required SOC level for i^{th} LAG to support ET among k^{th} EV and c^{th} CS. As measured time intervals are continuous in nature, we integrate energy units from 0 to desired SOC J_i^r. Computing L_{dis}^k provides us with exact information of energy units required for future trading with CS.

4 *EVBlocks*: A Blockchain-Based Secure ET Scheme for Electric Vehicles

Algorithm 1 *EVBlocks*: ET Algorithm

Input:EV wallet T_k exchange with CS, blockchain C_B, symmetric key E_{LG}, pseudo-random sequences ρ_k^n, and public/private key pairs of GS, denoted by χ_G.
Output: Energy traded bill units $\eta_{k_{A \to B}}$ for k^{th} EV charged by c^{th} CS in the i^{th} LAG, utility function U_k^j, and objective function o_k^j
Initialization: $i = 1, p = 1, c = 1, k = 1$

for $j \leftarrow i$ to n **do**
  for $k \leftarrow 1$ to n **do**
    for $i \leftarrow 1$ to p **do**
      $U_i^k \leftarrow (U_k^j \times B_i^k)/(p \times B_i^k) \times D_{k \leftarrow i/r}$
      $T_i \leftarrow \{I_{k \to c}^i, D_{k \to c}^i, nonce, C_{k \to c}^i\}$
      compute H_{prev}
    end for
    initialize $\rho_k^n \leftarrow (\rho_1, \rho_2, \ldots, \rho_k)$
    $L_s \leftarrow Session\_Initiate(G_k, \rho_k^n, nonce)$
    exchange session key k between LAG and GS.
    $E \leftarrow (E_{LG}[k, [C_B || G_k || L_k || \rho_k^n || Merkle\_Root]])$
    $H' \leftarrow H_{LAG} || C_B$
    $\chi_G \leftarrow \{Pub(G), Pr(G)\}$
    Perform asymmetric encryption E_{asm}/decryption D_{asm} as in equations 19 and 20
  end for
end for
for $i \leftarrow 1$ to n **do**
  for $k \leftarrow 1$ to p **do**
    for $c \leftarrow 1$ to q **do**
      $C_k \leftarrow \{ID_{EV}^k, P_{eu}, nonce\}$
      compute $H[C_k]$ as in equation 22
      initialize J_k^i
      $J_i^{req} \leftarrow (L_{i_SOC}^{max} - L_{i_SOC}^r) \times J_i^r$
      initialize Th_{min}
      $J_i^{av} \leftarrow (J_i^{req} + Th_{min})/p$
      compute L_{dis}^k as in equation 25
      $\eta_{i_{A \to B}} = L_{dis}^k \times \gamma$
      $\Delta f \leftarrow \{\Delta f1, \Delta f2, \ldots, \Delta fn\}$
      compute charging price $pk^{\Delta fi}$ as defined in equation 27
      $U_k^j \leftarrow Utility\_function(B_1^{req}, T_k, d(k, l))$
      $o_k^j \leftarrow max\ (U_k^j)$
    end for
  end for
end for

EVBlocks secures ET based on the a phased scheme. The phases in the proposed scheme are now discussed in the following subsections. Also, to facilitate the reader, the detailed nomenclature of the symbols used throughout the paper, is presented in Table 3.

4.1 *ETaaS*: ET as-a-Service via Edge Systems in SDN-Leveraged 5G-V2X Ecosystems

As discussed in Sect. 4, LAGs provide edge-computing services through ECC. Any TS *T* in ECC trades energy billing units, represented by η from any k^{th} EV for going from points *A* to *B* through SDN controlled switches. The transaction is represented as follows,

Table 3 List of Symbols

Symbol	Definition
r_i	Coverage range for i^{th} *LAG*
v_p	Set of p EVs within i^{th} LAG
V_k^i	Any k^{th} vehicle in a i^{th} LAG
U_k^i	Utility function to optimally select k^{th} node in i^{th} LAG
$D_{k\leftarrow i/r}$	Average latency for k^{th} EV to i^{th} LAG
C_B	Consortium Blockchain network
$I_{k\rightarrow c}^i$	Information units shared by k^{th} EV to c^{th} CS in i^{th} LAG
nonce	Unique random identifier
$D[EVs]$	discharging information of combined v_p EV units.
$C_{k\rightarrow c}^i$	Credits distribution by k^{th} node in i^{th} LAG
ρ_i^n	Pesudo-random sequence of i^{th} LAG, out of total n LAGs
C_k	Secret credentials to trade energy units by k^{th} EV in i^{th} LAG
P_{eu}	Energy price cost per unit
J_i^{req}	Desired SOC level of EV battery
L_{iSOC}^{max}	Maximum attainable SOC level
L_{iSOC}^{r}	Rated EV capacity
$\eta_{iA\rightarrow B}$	ET bill units from location A to B
J_i^{curr}	Current SOC level in i^{th} LAG.
$L_{i,SOC}^{req}$	SOC requirement of k^{th} EV in i^{th} LAG with c^{th} CS.
Δf	Slot length for a particular frame
$p_k^{\Delta fi}$	Price of charging EV k at a given slot Δf
p_k^s	Selling price of an energy unit to k^{th} EV
l_i^{opt}	Optimal edge charging node over set of all edge nodes
U_i^j	Utility function as defined in Eq. 31
c_i^j	Cost function for edge-service *ETaaS*
o_i^j	Objective function defined over the set of all LAGs L
τ^*	Game moves in non-cooperative game
ρ_i	Payoff mechanism for k^{th} EV
$\bar{C}_i$	Local convex optimization
e^*	Distinct and unique Nash equilibrium point in non-cooperative game model
C_i^j, D_i^j	Charging and discharging efficiency for k^{th} EV in j^{th} GS
C_L, D_L	Charging and discharging length
$P(t)$	Overall power consumption to determine rated capacity of EVs
T_{x_i}	Charging profile to achieve consensus
d	Local delegate from a set of delegates D

$$\eta_{i_A\rightarrow B} = L_{dis}^k \times \gamma \tag{26}$$

where γ denotes the units of energy exchanged. The LAG TS T regulates charging of a set of EVs $E = \{E_1, E_2, \dots, E_n\}$ where each $E_i \in E$ gets charged based on specified time slots, known as frames. These frames F are divided uniformly over a day length (24 hours). The slot length for a particular frame is denoted as Δf. For EVs $E = \{E_1, E_2, \dots, E_n\}$, the slots are represented as $\{\Delta f1, \Delta f2, \dots, \Delta fn\}$. EV charging is done by selecting a time frame $\Delta fi \in \Delta f$. The price of charging any k^{th} EV at a given slot is denoted by $p_k^{\Delta fi}$ and is represented as follows,

$$p_k^{\Delta fi} = \alpha\left(\frac{L_{iSOC}^{max}}{L_{iSOC}^{avg} - L_{iSOC}^{req}}\right) \tag{27}$$

s.t

$$0 > |\alpha| > 1 \tag{28}$$

$$p_k^s > p_k^b, if\, \alpha > 0 \tag{29}$$

$$p_k^s < p_k^b, otherwise \tag{30}$$

where p_k^s is the selling price of an energy unit to k^{th} EV and p_k^b is the buying price, respectively, $|\alpha|$ is the real-time market deviation in cryptocurrency *EnergyCoin* price. Measuring $|\alpha|$ smoothes out the sudden hike in price fluctuations [25]. Figure 4 depicts the overall network interaction of ET between CS and EV via LAG supported by edge services through ECC.To maximize the utility of energy transactions and minimize the latency, an optimal edge charging node l_i^{opt} is selected over the set of all edge nodes. l_i^{opt} provides the utility of edge-based peer ET service, termed as *ETaaS*, and is defined for k^{th} EV over the j^{th} optimal edge node as depicted in Fig. 5. The utility function is denoted as U_k^j and is calculated as follows,

$$U_k^j = \left(\frac{B_j^{req}.T_j}{(n+1).t_k^l}\right).\frac{1}{d(k,j)} \tag{31}$$

where $d(k, l)$ is the distance between k^{th} EV and j^{th} edge node. The cost function is defined as c_k^j and is calculated as follows,

$$c_k^j = B_j^{req}.U_k^j \frac{\partial d}{\partial j}[f(T_j, t_k^j.d(k,j)] \tag{32}$$

where B_j^{req} is the required bandwidth, T_j is the throughput provided by the j^{th} edge node, and t_k^j is the transactional delay. The function $f(.)$ is a three-input linear convex approximation cost function, with variables throughput, delay and distance. The aim is to maximize $f(.)$ w.r.t. j^{th} edge node. As distance $d(k, j)$ varies according to edge node location, we select constants k_1 and k_2 by equating $\frac{\partial d}{\partial j}f(.) = 0$. Plugging values of k_1 and k_2 in $f(.)$, we compute local maxima (i.e. $\frac{\partial^2 f}{\partial j^2}$ is negative). Similarly, to maximize the utility U_k^j, an objective function o_k^j is defined for set of LAGs $L = \{1, 2, \dots, l\}$ and represented as follows,

$$o_k^j = max[\sum_{j=1}^{l}(U_1^j\eta_1^j + U_2^j\eta_2^j + \cdots + U_l^j\eta_l^j]) \tag{33}$$

s.t

$$0 < U_k^j < U_{max} \tag{34}$$

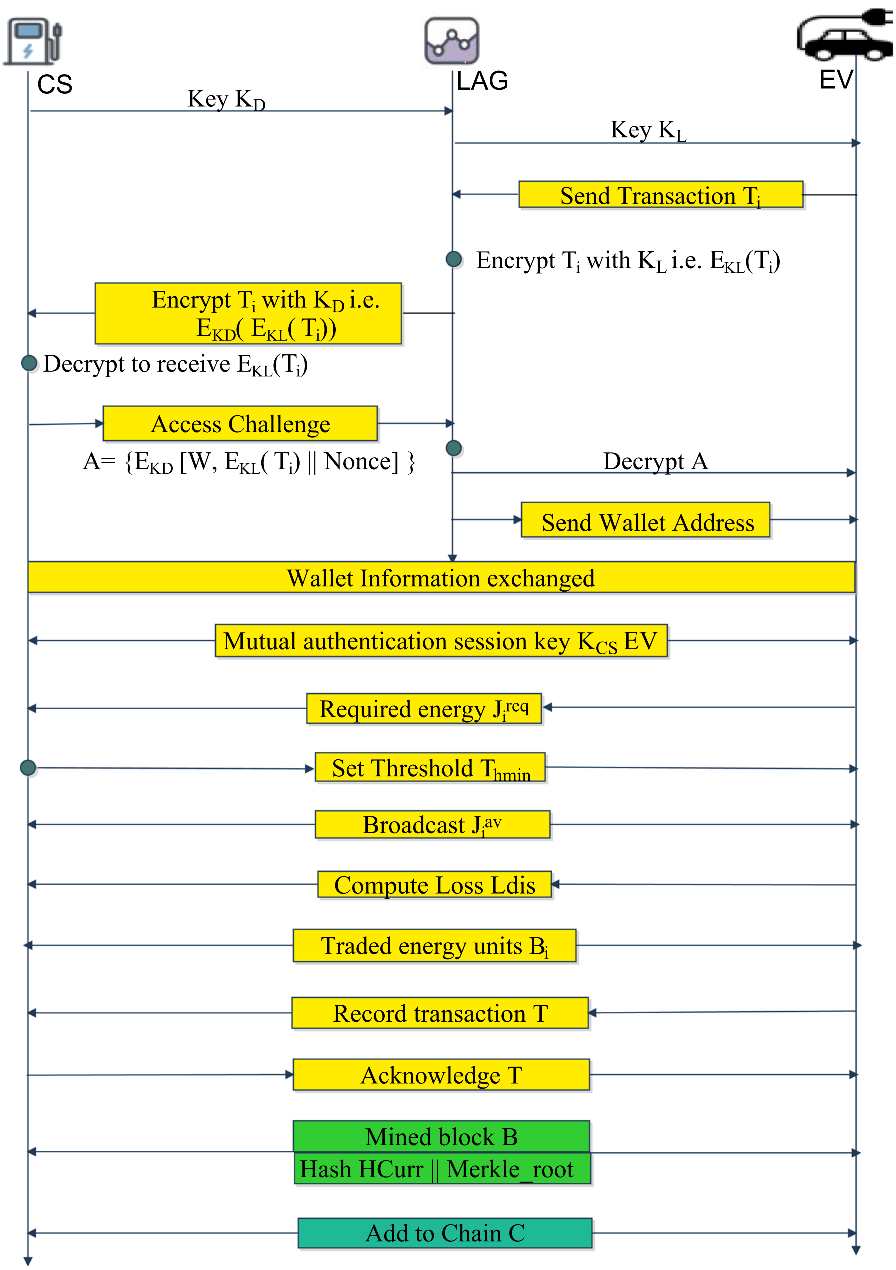

Fig. 4 Trading interaction between EVs and CS in *ETaaS* by utilizing services via LAG

$$0 < e_k^j < e_{max} \tag{35}$$

$$U_k(S) > U_k(b) \tag{36}$$

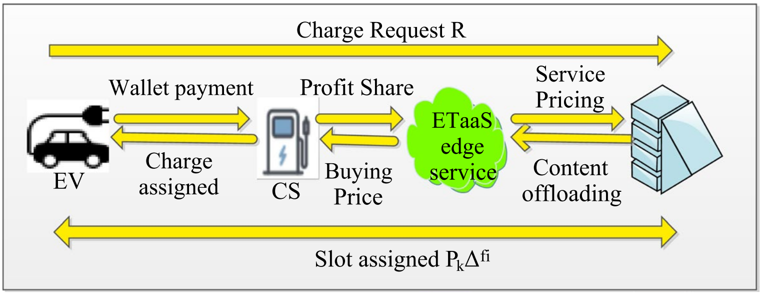

Fig. 5 *ETaaS*: ET as-a-Service

$$d_k(t) < d_k(t-1) \tag{37}$$

Based on the above discussion, we now present the ET Algorithm 1 that takes into account the interactions between CS and LAGs inside a GS G having public and private key pairs. The output is the energy bill units traded between EVs and CS, the utility function and the cost function of energy units traded.

4.2 *EVBlocks*: Proposed Non-Cooperative Game model

To maintain charging benefit of EV, E requests offloaded energy service over a set of LAG $L_i \in L$. To facilitate the same, a non-cooperative game N can be modeled based on energy units ω_i requested by k^{th} EV over an optimal selected offloaded LAG i. The offloading service is handled over a slot frame $F_i \in F$. At the initial phase, all the LAGs L_i determine the charging time slots Δf_i for k^{th} EV based on start time t_s, and forms a basis information b_i^k for i^{th} LAG providing offloading service to k^{th} EV. The game N has a set of possible actions $A = \{a_1, a_2, \dots, a_n\}$ and a set of possible strategies $S = \{s_1, s_2, \dots, s_n\}$ for each action $a_i \in A$. The mapping function is defined as $f : A \times S \rightarrow \{p_k^{\Delta f}, a_k^i, s_k^i, \tau^*\}$ where s_k^i denotes the k^{th} EV strategy to maximize profit with the i^{th} LAG during trading, and τ^* denotes the set of all possible moves (transitions) in the game N. The non-cooperative game N is modeled as follows,

$$N = \{P, A, S, \tau^*, p_i^{\Delta f}, \rho\} \tag{38}$$

where P denotes the set of players (EV and CS) in the game, $p_i^{\Delta f}$ denotes the allocated price decided by the game moves τ^*, and $\rho_k \in \rho$ denotes the payoff mechanism of k^{th} EV for energy traded units. The actors in the game are as follows.

Algorithm 2 *EVBlocks*: Non-Cooperative game

Input: set of EVs $e_k \in E$, LAG $L_j \in L$, frames $F_k \in F$, ρ_k, moves τ^*
Output: Space state tree T having a unique and distinct Nash equilibrium e^*
Initialization: $k = 1, j = 1, i = 0$

for $k \leftarrow 1$ to k **do**
  for $j \leftarrow 1$ to l **do**
    $t_s \leftarrow slot\_initialization(\Delta f_k, t_s, b_{j,k})$
    $A \leftarrow \{a_1, a_2, \ldots, a_m\}$
    $S \leftarrow \{s_1, s_2, \ldots, s_p\}$
    $f \leftarrow \{p_k^{\Delta f}, a_k^j, S_k^j, \tau^*\}$
    $p_k^{\Delta f} \leftarrow max(o_k^j, p_k^s, p_k^b)$
    compute c_k^j as defined in equation 32
    $\rho_k \leftarrow -c_k^j$
  end for
end for
$i \leftarrow i + 1$
while $(N == e^*)$ **do**
  for each LAG j **do**
    $\tau* \leftarrow \{\tau_1, \tau_2, \ldots, \tau_i\}$
    if $(a_i \times s_i$ maps to $\tau_i)$ **then**
      $p \leftarrow Compute\_Path(p_1, p_2, \ldots, p_l)$
      add p to solution set of Tree T
      $L_{-i}^{k-1} \leftarrow \{L_{\tau_1}^{k-1}, L_{\tau_2}^{k-2}, \ldots, L_{\tau_k}^{0}\}$ at previous state $(k-1)$
      $L_{-i}^{k} \leftarrow \{L_{\tau_1}^{k}, L_{\tau_2}^{k-1}, \ldots, L_{\tau_k}^{1}\}$ at current state (k)
      $\kappa \leftarrow |L_{-i}^{k} - L_{-i}^{k-1}|$
      if $(\kappa \leq \Phi)$ **then**
        $Add\_path(L_{\tau_1}, L_{\tau_2}, \ldots, L_{\tau_k})$
      else
        mark as **invalid path** and add to $\overline{\mathrm{p}}$
      end if
    else
      output error "*State not found for transition* τ^* *and exit*"
    end if
  end for
end while

- **Players** P: $\forall e_k \in E$, and $\forall l_j \in L$ denotes the EVs (buyers) and CS (sellers).
- **Actions** A: $\forall a_k \in A$, determine t_s and basis information b_j^k.
- **Strategy** S: $s_k \in S$ to maximize the pay utility U_k^j subject to constraints as defined in Eq. (38).
- **Moves** τ^*: Set of all state transitions moves that deterministically starts from an initial action state a_0, takes a label strategy transition over possible strategies S, to converge to a final action state a_f.
- **Price** $p_j^{\Delta f}$: Consists of selling price of energy units by CS, denoted as p_j^s and buying price of energy units by EVs, denoted by p_k^b. The objective is to maximize the function o_k^j subject to constraints defined in Eq. (38).

– **Payoff** ρ_k: A payoff scheme ρ is designed for any EV supported by agreegator LAG $l_j \in L$. ρ_k is defined as follows.

$$\rho_k = -c_k^j = -[B_j^{req}.U_k^j \frac{\partial d}{\partial j}[f(T_j, t_k^j.d(k,j)]] \tag{39}$$

The game N operates over moves as sequence of state transitions $\tau^* = \{\tau_1, \tau_2, \dots, \tau_w\}$. Let $\tau_q \in \tau^*$ be a possible general move for LAG l and EV e. Depending on the transaction profiles generated by the ESP server T, τ_q maps $a_q \times s_q \rightarrow \tau_q$. The incorrect moves are marked as transition to a dead state D and contains the complement of moves in τ^*, and is denoted as $\overline{\tau^*}$. Depending on the actions and strategies to maximize profits, we construct a tree T having root node as T_{root}, which is initially an empty set ϵ. The winner W of the game adds a newly created child node to parent T_{root} via an edge e. The tree grows by adding nodes $\{n_1, n_2, \dots, n_p\}$ and edges $\{e_1, e_2, \dots, e_p\}$ by selecting moves $\{\tau_1, \tau_2, \dots, \tau_p\}$. The local convex optimization $\overline{\mathrm{C}_k}$ [14] is represented as follows,

$$\overline{\mathrm{C}_k} = argmax\{C_k(C_k, C_{-k})\} \tag{40}$$

where $\{C_k(C_k, C_{-k})\} \equiv v_k^j$ and C_{-k} is the EV payoff principle ρ_j for set of LAG aggregators $l_j \in L$.

Proposition 1 *The set of moves τ^* in the game N has a unique and distinct Nash equilibrium e^*.*

Proof For a given C_{-k}, the local optimization $\overline{\mathrm{C}_k}$ is concave and is a Hermitian Matrix H_k [44] over the set of utilities U_k^j and is strictly negative. The distinct actions $a_k \in A$ are based on strategy set S that defines a payoff ρ_k which is distinct and non-empty. The transitions states are deterministic over the tree T by adding an edge, iff $\tau_q \in \tau^*$ exists. Hence, there exists a pure Nash equilibrium strategy [39]. The Nash equilibrium for the game N is $e^* = \{e_1, e_2, \dots, e_n\}$ and can be found by traversing tree T using Depth first search (DFS) strategy. The equilibrium terminates when the relative distance between two consecutive iterations j_k and j_{k-1} is small by a relative factor Φ, i.e., $|\chi^{j_k} - \chi^{j_{k-1}}| \leq \Phi$. □

Proposition 2 *The nash equilibrium e^* for the set of all moves τ^* has a perfect equilibrium for the game N.*

Proof Since the game N is modeled as a tree space T, we traverse from T_{root} and reach node n_j. The sub-moves τ_s^* to n_j are those path lengths $P = \{p_1, p_2, \dots, p_j\}$ where any edge $p_k \in P$ has a valid transition move defined in τ^*. Hence, the outcomes of the edge transitions maximize the utility U_k^j and minimize p_k. The remaining paths $\overline{\mathrm{p}} = \{p_u, p_{u+1}, \dots, p_s\}$ are invalid and does not reach a unique equilibrium state. Hence, they are not added to the solution set by DFS. Thus, for a given Nash Equilibrium that is distinct over τ^*, there exists a perfect equilibrium for the game N.

The non-cooperative game is depicted in Algorithm 2. As k EVs request energy units over slot charging slots Δf_i, the space complexity for maintaining slot information is $O(kl)$. Also, the game N operates by a selection of state moves τ^* over n LAGs for p EVs. Thus, the time-complexity of algorithm 2 is $O(p.n.\tau *)$. $\square$

4.3 *PoG*: A consensus Serial Event-Driven Algorithm for *EVBlocks*

Consider the set of transactions $T = \{T_1, T_2, \dots, T_n\}$ operating between EVs and CS modelled over game N. The power supplied from GS is maintained as a local state function ϱ and is used for charging/discharging of EVs. The state function defined as $\varrho_i = \{\varrho_1, \varrho_2, \dots, \varrho_n\}$ denotes the charging rate c^j_k for k^{th} EV and j^{th} GS and is given as follows,

$$C^j_k = v \sum_{k \in C_t} x^j_k \tag{41}$$

where v is the charging efficiency based on properties of electrical conductor and x^j_k is the operational charged energy state of k^{th} EV managed by j^{th} GS during operational time C_t. Similarly, the discharging rate D^j_k is represented as follows,

$$D^j_k = \omega \sum_{j \in D_t} u^j_k \tag{42}$$

where ω is the discharging efficiency and y^j_k is the operational discharged energy state and excess energy transferred back to j^{th} GS over discharging time d_t. The k^{th} EV starts charging at time t^s_k and finishes at time t^f_k, hence the charging length is C_L is denoted as follows.

$$C_L \leq max(U^j_k(t^s_k - t^f_k)\frac{\partial d}{\partial j}(f(L^{max}_{jSOC}, c^j_k, T_j) \tag{43}$$

Similarly, the discharging length D_L is calculated as follows.

$$D_L \leq min(U^j_k(t^s_k - t^f_k)\frac{\partial d}{\partial j}(f(L^{min}_{jSOC}, c^j_k, T_j) \tag{44}$$

Charging length denotes the battery capacity of EVs. The overall power consumption is represented as follows.

$$P(t) = \int_{t \in T} (C_L - D^j_k)dt + base(t) \tag{45}$$

where $base(t)$ is the base power consumption to dampen electrical fluctuations in the network. The optimization is defined as C^{max}_L, and D^{min}_L and is denoted by O^j_k, and defined as follows.

$$O^j_k = \int_0^T (P(t) - P(t-1)^2 dt \tag{46}$$

s.t.

$$\int_{t_k^s}^{t_k^f} U_k^j \geq C_k^j, (k,j) \in \{1, 2, \ldots, N\} \tag{47}$$

$$\int_{t_k^s}^{t_k^f} U_i^j \leq D_k^j, (k,j) \in \{1, 2, \ldots, N\} \tag{48}$$

The charging profile $T_{x_k} = \{C_k^j, D_k^j, C_L, D_L, O_k^j\}$ for k^{th} EV performing energy transaction with j^{th} CS is communicated to GS via a local delegate $d \in D$. d assigns T_{x_k} to an event-driven scheduler S. S provides a serial-driven event schedule based on a locally c-competitive convex optimization problem [34]. To achieve it, the scheduler divides time frames Δf into discrete transfer slot units denoted as $t_{k,m}$ where k denotes the EV number and m denotes the input line for EVs. The slots are numbered as $\{1, 2, \ldots, l\}$. Slots are differentiated on the basis of successful and collision slots. Any l^{th} slot is successful if k successfully sends an energy transaction packet from input line m to leader EV_L, and other nodes do not transmit in l^{th} slot. Otherwise, in case of contention between two EVs p and q for slot l, it indicates a collision slot. The output of the contention is stored in S. Based on the output of S, the delegate $d \in D$ forms a global and local consensus among transactional added to nodes. All EVs are now in contention for energy frame transfer via these common slots length L_s. To minimize collisions, a 0.01-persistent carrier sense multiple access (CSMA) is provided. Successful slots

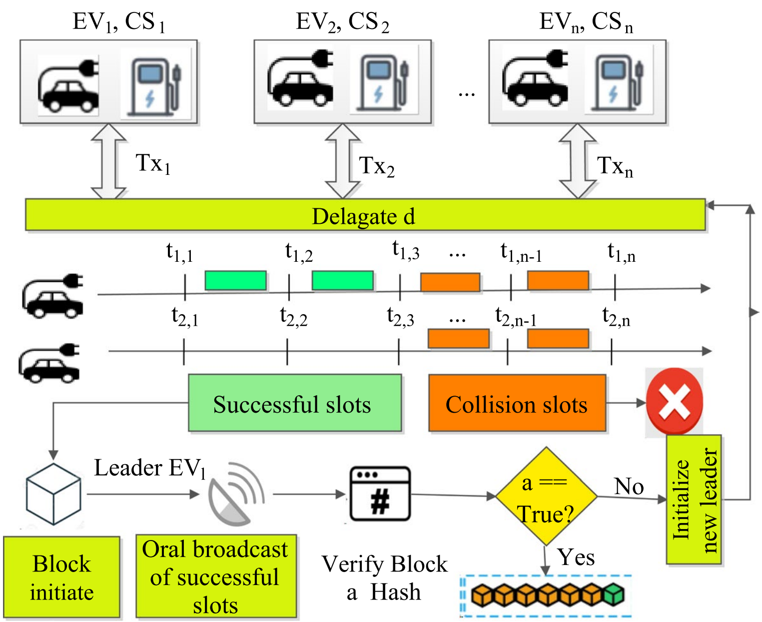

Fig. 6 *PoG*: Proof-of-Greed Consensus mechanism

are then communicated via local coordinator β elected through the proposed consensus mechanism *PoG* among all EVs as depicted in Fig. 6.

Algorithm 3 *EVBlocks*: Distributed Consensus Algorithm

Input:Transaction set $T = \{T_1, T_2, \ldots, T_n\}$, previous block hash H_{prev}, local state S_i for i^{th} block, local coordinators L for message exchanges.
Output: Oral broadcast of new block mined B_{new} to set of all nodes N
Initialization: $\mu = 0, q = 1$, and height h of blocks

1: **for** each delegate $d \in D$ **do**
2:     **for** each transaction $T_x \in S$ **do**
3:         **if** (Verify$T(t_x)$ == TRUE) **then**
4:             $A_{tx} \leftarrow$ assign(Tx)
5:         **else**
6:             $S_m \leftarrow S_{tx}$
7:         **end if**
8:     **end for**
9:     $\alpha \leftarrow \textit{Block\_Initiate}(S_m, D_m)$
10:     $\beta \leftarrow \textit{initialize\_leader}(T_1, T_2, \ldots, T_n)$
11:     **if** $(m == \beta)$ **then**
12:         $\textit{Broadcast\_Consensus}(A_{Tx}, h, \mu, q, \alpha, sig_{S_{k_q}}(H(\alpha)))$
13:     **else**
14:         $E \leftarrow \textit{Error\_Notification}(T, H_{curr}, S_i, L_{curr})$
15:         $\textit{Notify\_EV}(T, H_{Tx}, E)$
16:         print"**Block not mined**"
17:     **end if**
18: **end for**
19: **for** $d \in D$ and $d \neq \beta$ **do**
20:     **if** (Verify_Block(α)== FALSE) **then**
21:         $\mu_q \leftarrow \mu + q$
22:         $\textit{Broadcast}(L, h, \mu, d, \mu_q)$
23:         **if** (count$(\mu_q) \geq M - f$) **then**
24:             $\mu \leftarrow \mu_q$
25:             $\mu \leftarrow \textit{Initialize\_New\_Leader}(T_1, T_2, \ldots, T_n)$
26:         **else**
27:             $q \leftarrow q + 1$
28:             GOTO **Step 2**
29:         **end if**
30:     **end if**
31: **end for**

The election procedure is based on the current value of traffic profiles of EVs that might change once excess energy is transferred back to GS. A traffic profile for any k^{th} EV contains transaction information T_k. Hence, the election process is termed as *greedy* w.r.t. scheduler S as local consensus may not lead to a global consensus state. β then broadcasts the successful slots as follows,

$$B = \{A_{T_x}, h, \mu, H_{curr}, q, \alpha, S_k, L_{curr}\} \tag{49}$$

where A_{T_x} are assigned transactions, h denotes the current block height, H_{curr} is current block hash, q is a counter for managing re-transmissions (in case of collision slots), μ is saturation cutoff range, and $sigs_{q_m(H(\alpha))}$ is signature operation on α. The EVs are notified of unsuccessful transmission as follows,

$$\phi = \{T, H_{T_x}, E\} \tag{50}$$

where E denotes the serial identifier of EV signed by $sigs_{q_m(H(\alpha))}$. In algorithm 3, *initialize_leader* function elects a leader EV_L based on EV that has maximum number of successful transactions appended to chain. The leader is now appointed as local coordinator β to facilitate consensus. Once β is selected, the height h of blocks is increased by 1, and signature parameters defined in Eq. 49 are computed. The details are then broadcasted in the network through a simple broadcast address, as defined in *Broadcast_Consensus* function. If no leader is appointed, function *Error_Notification* with inputs as $\{T, H_{curr}, S_i, L_{curr}\}$ is broadcasted to roll-back the election process to local state S_i. L_{curr} denotes the current length of chain at the instant. All participating EVs are notified through *Notify_EV* function. The parameters are mentioned in Eq. 50. The EVs whose slots have collided need to broadcast their energy frame as unsuccessful attempts. The leader EV_L selected by β then verifies block-hash $H(a)$ and adds it to the chain. At all times, the height h of the chain length is also stored as to purge same-length chains created via forking operations. If block verification fails, then cutoff μ is increased by μ=$\mu + q$, denoted as μ_q, and the count is maintained as $count(\mu_q)$. An objective load function f is designed to minimize re-transmissions.To comply with this, cutoff $\mu_q \geq M - f$, where M is the message length. If conditions fail, the collision slot is considered for re-transmission, and counter q is incremented, and the entire process is then repeated. The details of the consensus mechanism are now presented in Algorithm 3.

5 Performance Evaluation of *EVBlocks*

In this section, we evaluate the performance of *EVBlocks* based on two factors. First, we present the obtained simulation results based on the adaptive charging network (ACN) EV dataset [31], to study the EV behaviour. The dataset consists of over 30,000 EV charging sessions from two CS sites, geographically located in California. The dataset is managed by PowerFlex, which is an EV charging startup. Next, based on the analyzed EV charging profile behaviour, we present the simulation parameters for the experimental setup and evaluation process.

5.1 ACN-EV Dataset

The dataset consists of charging profiles of 54 EV supply units, or CS), located at the Caltech campus in California. The CS contains a 50 kilowatt DC fast charger and includes the charging profile details of parked EVs throughout the day. EVs are charged to full capacity through an adaptive scheduling algorithm, and rated battery usage is measured. The dataset consists of field descriptors like EV *cluster_ id*, *charging_current*, *user_ID*, *connection_ID* for charge transfer, and *charging_duration* (connect and disconnect time).

5.2 Plots of EV Charging Profiles

To begin the simulation, we import the *acnsim* library in Python, and set up the Caltech timezone, and kept the charging interval setup for 5 minutes. The network voltage is set to 220 volts. We first set the default maximum charging rate of EV battery as follows,

$$C_{max} = 32 \times V/100 \tag{51}$$

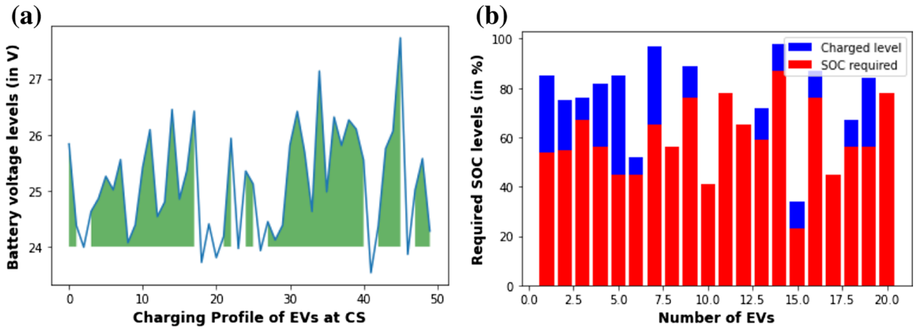

Fig. 7 SOC and Charging profiles of EVs-ACN-charging dataset: **a** Voltage levels of EVs during charging, and **b** Required and utilized SOC levels of EVs

where C_{max} is the default battery power. Next, we set up the charging network with a defined constraint matrix representing the electrical wire interface in the dataset. The network is manually configured through the *add_constraint()* method, *register_EV()* method, and *charge()* method. Next, we set up the event-driven charge scheduling through *acn-data_events* package that simulates the real EV behaviour. The library is accessed through a token-based API. A scheduling algorithm is presented in *acnsim* that allows dynamic scheduling of EVs for charging-based slots at CS. We present the plots for SOC and charging profiles of EVs. Figure 7 depicts the plots. We consider a total of 50 nodes (EVs and CS) that perform ET over a day long. We measure the aggregate battery levels of EVs and CS during the transaction. As through *PoG*, we measure $P(t)$, and set $base(t)$ at 24 V. Based on charging profiles T_{x_k}, and slot lengths, we dampen the charge fluctuations for both EVs and CS. Figure 7 (a) presents the details. We only observe a charge shoot beyond 27 V, and a minimum shoot below the threshold level of 24 V. Most of the charge fluctuations are balanced in the range, which indicates that event-driven simulation balances the voltage loads. Next, we measure the ET scenario and measurement of SOC levels for 20 EVs. Figure 7 (b) presents the EVs energy levels and charging requirements of batteries when traded exchange occurs with CS. As indicated, we present the SOC requirements of EVs and the present charge levels of EVs.

In some cases, the EVs are required to consume all the presented battery (complete red bars), and some have excess energy (blue with red bars) that can be traced back to the ecosystem. Based on the SOC levels, the difference between the required and present charge levels is highlighted. In most cases, the edge services handle most of the requests and form a resilient exchange. The ET transactions are recorded in BC, and the recycling fluctuations are minimized through the proposed event-driven consensus [30].

We now present the key analysis of the derived EV plots. Figure 8 (a) presents the energy transacted between CS and GS profile for a single day (24 hours). From the figure, it can be inferred the max-peak load range of $0.8 - 0.9$ is achieved between 6:00 and 9:00 AM (morning), and the load significantly reduces to 0.15 between 12:00 noon and 3:00 PM. The load significantly drops as most EVs are parked after usage at evening hours. Thus, from the simulation, it can be inferred that EVs sufficiently trade energy with CS and GS at day-hours, and thus, responsive ET services at the edge are required. The edge nodes can be switched to *SLEEP* mode once the EVs are parked, as ET transactions decrease gradually. Next, we present the utilized current or total aggregate current of EV over a

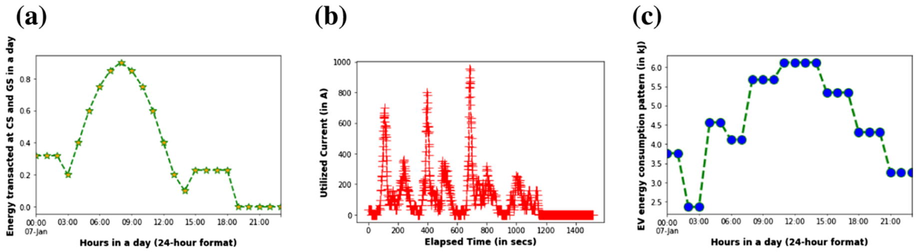

Fig. 8 Charging plots for EVs from ACN-charging dataset: **a** Transacted enegy between CS and GS (single day profile), **b** Utilized current by EV during charging, and c EV energy consumption profile (single day profile)

specified time interval. Figure 8 (b) presents the details. The simulations show that EV has a peak aggregate of 981.6 ampere (A) at the elapsed period between $650 - 725$ secs. As more time elapses, the current utility of EV gradually decreases and eventually drops to base level after 1200 seconds. Thus, the plot presents useful insights into EV SOC levels. After a specified time threshold, the proposed scheme maintains a charging set E of EVs and presents time intervals as slot lengths Δf_n. Once L_{SOC}^{req} falls below the threshold, EVs have to start ET with the nearest LAG, and it invokes a non-cooperative game among EVs and CS for profit maximization.

Next, we present the EV energy consumption profile over a day. The details of the same are presented in Fig. 8 (c). As evident, EVs maximum energy, $\approx$ 6.25 kJ, during the daytime slot. This validates the load assumption presented in Fig. 8 (a), as more EVs run out of charge and thus perform ET with CS. Thus, the energy transaction among CS and GS approaches maximum load during the daytime. The excess charge/discharge units can be supplied back to the sink through our proposed event-driven consensus scheme, which takes into account C_L, and D_L respectively, and dampens the charge fluctuations over base power consumption (or average load behaviour).

Based on observed EV and GS charging and load profiles, we present the simulation parameters for the EV setup. The details of the same are presented in Table 4. These parameters are chosen on the basis of ET [11, 57], measurement of SoC levels [12], minimizing block latency [24], and maximizing profits by non-cooperative game approach [44]. We assume that most of the edge nodes are available in the desired spatial range and are uniformly distributed over the given map region to minimize latency. The pricing utility is modelled to minimize high fluctuations, where α is selected based on observed standard rather than mean deviation. We compare the performance of *EVBlocks* with conventional(flat) and fixed tariff schemes [47] in blockchain. In the conventional or flat scheme, the base unit price per unit P and the charged fee are the same for all transacting EVs with CS. In fixed-tariff scheme, a non-cooperative game model among players EVs and CSs with energy demand modeled as a linear function $\pi(\theta)$ given as $\pi(\theta) = cx(\theta) + Z$, where c is a constant fixed for transactional consensus, and x is any k^{th} EV.

5.3 Experimental Setup

The setup deploys open-source confidential consortium scheme (CCF) [1] *v1.0*. The path libraries are set on a virtual machine (VM) running Ubuntu Linux *v18.04* LTS with two

Table 4 Simulation Parameters

Parameters	Values
E: Total number of EVs e	35
LAG: l	2
CS: c	10
η: Mined energy transactions	0-3000
T: TS	1
h: hours (in a day)	0–24
U_i^j: i^{th} EV utility with j^{th} edge node	ordinal scale 1–6 *1: low utility, 6: excellent*
T_s: Transactions performed over TS T	2800
L_{iSOC}^{r}: rated battery capacity	27kW
L_{iSOC}^{req}: SoC levels (in mW)	10–38mW
p_k^s: selling price of energy unit (1kwH)	1.4 \$/kwH
p_k^b: buying price of energy unit (1kwH)	0.7 \$/kwH
α: constant to smoothen load in price fluctuations	0.4
k: iterations performed to maximize profit	0-16
C_b: Block transactions in CBC	0–1000
v: Charging efficiency	0.8
ω: discharging efficiency	0.4
β: charging iterations	20–200
θ_t: max collision throughput (CSMA/CA, $p = 0.01$)	0.84

Table 5 Types of EV

EV_Type	Max battery capacity (in kwH)	Charging voltage (in V)	Internal resistance (in Ω)
1	32	220	6.875
2	18	210	11.666
3	22	240	6
4	62	325	3.823
5	8	110	7.333

virtual CPU cores. The internal memory is 4 GB RAM with 30 GB external hard-drive. The testing is performed on Node.js *v8.9.1* with npm *v6.7.0*. For the SDN controller switch, we have used OpendayLight Controller Neon-SR1 to manage server hyper-visors.

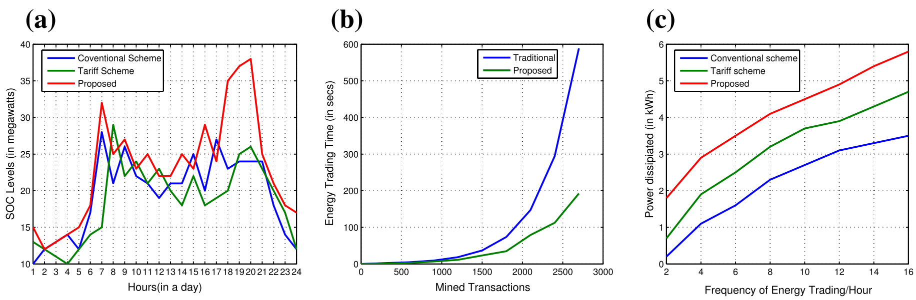

Fig. 9 Performance analysis for ET: **a** Measurement of SoC charging levels , **b** Energy Trading time vs Mined Transactions, and **c** Power dissipated (in kWh)

5.4 EV Setup

A sample area map distributed over a 20km spatial range is selected. The scenario considers 2 LAGs L operating over the range to support ET between 5 different types of EVs with 7 EVs in each type. The total number of CS is 10. EVs can supply excess energy back to CS and vice-versa, with an operational up-time of a day length (0-24 hours). The performance of EV output is measured by fixing Th_{min} w.r.t. simulation parameters as listed in Table 4. The specifications of EV type are presented in Table 5.

5.4.1 Performance Analysis of ET

EVs trade excess energy to CS or require energy from CS. The energy profiles of EVs types are loaded, and SoC levels are measured for the proposed scheme, as shown in Fig. 9 (a). It can be inferred that as the number of hours increases, the proposed scheme maintains an average SoC charge of 22.8MW, with a peak of 37.5 MW, which is 25% higher than other approaches. The decay in the proposed approach is also graceful at 17.4 MW. As more EVs are charged based on specific time frames, with frame length Δf, the charging is fast as we only need to refer to the index of the frame unit. Fig. 9 (b) shows the various values of η w.r.t. the block trading time B_t. At 1000 transactions, the value of B_t for both proposed and conventional methods is $\approx$ 12.06 secs. At 2750 transactions, the difference is $\approx$ 396.97 secs, with a significant decrease of 67.3% in the proposed approach. As trading nodes are closer to the edge and employ content offloading services, the trading time is minimized. In Fig. 9 (c), we have compared our proposed approach against two conventional schemes: tariff scheme and conventional (flat) schemes. The figure indicates that the average power dissipation of the proposed scheme is 4.1125 kWh, compared to 3.1127 kWh for the tariff scheme and 2.225 kWh for conventional methods. The peak power dissipated is 5.8kW at 16 energy transactions/hour among EVs. This peak is 29.31% higher than the combined approaches. As the objective function considers maximizing the utility function, more energy transactions can be performed. Thus, EVs can supply more excess energy back to CSs or GSs, indicating higher satisfaction of EVs.

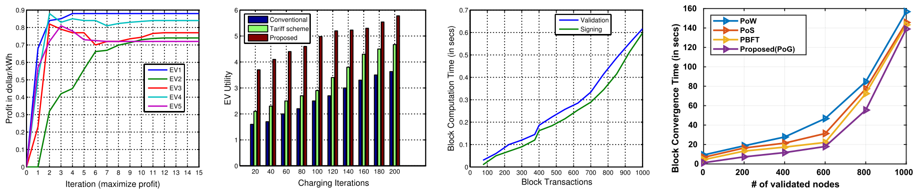

Fig. 10 Impact of Non cooperative game and consensus mechanism *PoG*: **a** Profit in \$/kwH for charging EVs, **b** Utility of EVs , **c** Block computation time (in secs), and **d** Block Convergence Time (in secs)

5.4.2 Impact of Non-Cooperative Game in Maximizing Profits

The proposed non-cooperative game N assumes mapping between actions and strategies and designs a payoff function based on the defined cost function. The incorrect transition moves are discarded, and the space search tree is built based on moves τ^*. To simulate this, we assume different types of EVs with specifications, as depicted in Table 5. The profit function is measured between two consecutive iterations $(k-1)$ and k over slot length of Δf. The following is depicted in Fig. 10 (a). It can be inferred that initially, as the game moves are built, the profits are maximized for all EV types as the margin of p_k^b and p_k^s is high, but gradually the profit margin becomes constant for all EVs. The final stable profit values for $EVs = \{EV1, EV2, EV3, EV4, EV5\}$ are (0.88, 0.74, 0.77, 0.84, 0.72) respectively. The stable values indicate that search space for tree T is built and any path of the tree $\{p_k, p_{k+1}, \ldots, p_l\}$ will lead to the same node at the final iteration following the defined path. This proves the existence of nash equilibrium e^* for all EV types.

5.4.3 Performance of Consensus Mechanism *PoG*

To measure the performance of event-driven by *PoG* consensus algorithm, we compare the results against tariff and conventional schemes, as depicted in Fig. 10 (b). The proposed scheme has an average utility value of 4.883 compared to 3.317 for the tariff scheme and 2.613 for the conventional scheme. Thus, the proposed scheme achieves higher utility by a factor of 1.64. As successful slots are higher, more blocks are hashed to be added to the chain, resulting in more EV utility. To minimize fluctuations during charge supply, we set charging and discharging parameters v and ω as depicted in Table 4. Figure 10 (c) shows the block computation time for signing operations using symmetric key k_m over a hashed block. As blocks are increased, the signing time increases slowly with an average value of ≈ 0.236 seconds for 1000 transactions. The average value of validation is ≈ 0.2722 seconds. As collision slots are minimized based on optimization function o_i^j, only successful transmission slots are communicated via block leader EV_l resulting in less block computation time. Figure 10 (d) validates the advantage of proposed consensus mechanism *PoG* against other conventional consensus protocols. We consider an additional parameter *’block convergence time’* as the time required by all nodes to agree on the same truth, i.e., consensus vs. validated blocks via consensus. A node may contain a set of energy transactions $\{E_1, E_2, \ldots, E_n\}$. The results favour *PoG*, and it outperforms the said approaches for small values of mined nodes. At 200 nodes, the average converge time of conventional schemes is 16.10 secs, and the proposed is 7.27 secs. As the number of nodes increases, the difference of block convergence time reduces against conventional schemes. At 1000 nodes, the average of conventional schemes is 148.56 secs, compared to 138.96 secs in *PoG*. As

Table 6 Computation and communication cost of various identifiers

Identifier	CC (in seconds)	CCM (in bits)
ID_i	0.00032	32
E_{sym}	0.0056	32
E_{asym}	0.0215	32
nonce	0.00032	16
$H(ID_i)$	0.00032	160
H_m	0.00032	256
S_m	0.004085	192
V_m	0.005865	192
T_i	0.00032	160

ID_i: Identity cost; E_{sym}: Symmetric encryption cost ; E_{asym}: Asymmetric encryption cost; *nonce*: random nonce cost;$H(ID_i)$: Hash for fixed identity cost; H_m: Message hash; S_m: Message Signature cost; V_m: Message verification cost; T_i: Transaction appended to chain cost;

PoG elects local coordinator β based on slot-lengths, the scheme is not scalable for a large number of nodes. However, *EvBlocks* exploits edge services through *ETaaS*, hence energy transactions are locally resolved. This allows proper load-balancing among all LAG servers. So fewer transactions are present at the local coverage range, thereby making *PoG* as optimal consensus protocol w.r.t. the limiting conditions.

5.5 Security Evaluation of *EVBlocks*

The proposed scheme is now evaluated for the secure and private transfer of EV identities over the CBC C_B. To perform security computations, the computation costs (CC) and communication costs(CCM) of security identifiers are taken from [45]. Table 6 depicts the CC and CCM of various identifiers as presented in [45].

5.5.1 Computation cost

The computation cost is evaluated in three phases. Firstly, EVs perform ET with CS as proposed in Algorithm 1. The proposed algorithm consists of a wallet T_i exchange, symmetric key operations between EVs and CSs, and asymmetric key operations based on public/private pairs of GS. The ET algorithm consists of 5 hash operations, two symmetric key operations, and one asymmetric operation. Thus, the time required is $5 \times 0.00032 + 2 \times 0.0056 + 0.0215 \approx 0.0343$ seconds. Secondly, the profit margin of EVs is maximized based on the non-cooperative game as depicted in Algorithm 2. The algorithm consists of 2 block transaction appends. The cost required is $2 \times 0.00032 \approx 0.00064$ seconds. Finally, the consensus mechanism is framed to minimize energy fluctuations while transferring excess energy of EVs back to GS, as presented in Algorithm 3. The algorithm contains three hash operations; two transactions append operations, one signing and one verifying operation. The cost required is $3 \times 0.00032 + 2 \times 0.00032 + 0.004085 + 0.005865 \approx 0.011350$ seconds. Thus, the overall computation cost for the proposed scheme is $0.0343 + 0.00064 + 0.011350 \approx 0.046290$ seconds or 46.92 ms.

Table 7 Comparison of overall computation (CC) and communication cost (CCM) against existing schemes

Scheme	CC	CCM	ME
Odelu *et al.* [37]	$7E_{asym} + 12H_m + 2T_{pair} \approx 505.72ms$	240 bytes	3
Hathaliya *et al.* [17]	$9H_m + 3E_{sym} + 4E_{asym} \approx 96.64$ ms	176 bytes	3
Proposed *EVBlocks*	$8H_m + 2E_{sym} + E_{asym} + 3T_i + S_m + V_m \approx 46.92$ ms	149 bytes	8

E_{asym}: Asymmetric encryption cost; H_m: Hash output cost; T_{pair}: Bilinear pairing cost; E_{sym}: Symmetric encryption cost; T_i : Transaction append cost; S_m: Signing cost; V_m: Verification cost

5.5.2 Communication Cost

The communication cost is evaluated in the same pattern of computation costs. Firstly, the ET algorithm 1 between EVs and CSs performs a wallet transaction exchange, one session key exchange, one certificate issue to verify credentials of q^{th} CS in i^{th} LAG, and one encryption and decryption operation. Thus, the total bits involved in communication is $160 + 32 + 256 + 32 + 32 = 512$ bits. Then, the non-cooperative game algorithm 2 exchanges information of time slot Δf. Considering 100 frames, the total exchange is 100 bits. The mapping operation $a_i \times s_i \rightarrow \tau_i$ takes 32 bits exchange, then 16 iterations are performed for path addition to tree T, each path takes 1 bit information. So, 16 bits are required. To check the added move, $\tau \in \tau^*$ is valid/invalid, 1-bit check flag information is appended. Thus, total bits are $100 + 32 + 16 + 1 = 149$ bits. At last, the consensus *PoG* algorithm 3 requires verification of transaction T_x, i.e., 192 bits, block creation takes 160 bits, consensus broadcast message requires 160 bits, and the corresponding EV is notified, which requires 1 bit. Then, considering leader selection for 16 iterations, leader selection β requires 16 bits. Finally, slot identification as success or collision requires a flag of 1 bit. Thus, total communication cost is $192 + 160 + 160 + 1 + 16 + 1 = 530$ bits. Thus, the overall communication cost of the proposed scheme *EVBlocks* is $512 + 149 + 530 = 1191$ bits or 149 bytes of information. The number of message exchanges (ME) in ET algorithms are one for session exchange and one for certificate exchange, so the total is two messages. In the non-cooperative game path addition and flag information, a total of 2 messages, and in *PoG* algorithm, there is consensus broadcast, Notify_EV, leader selection, and slot collision, i.e., a total of 4 messages. Total messages exchanged are $2 + 2 + 4 = 8$ messages. Table 7 shows the overall comparison of Computation cost (CC), Communication Cost (CCM), and several messages exchange (ME) against existing schemes.

5.6 Efficiency of *EVBlocks* Against Conventional Schemes

The proposed scheme *EVBlocks* is now compared against existing state-of-the-art schemes. *EVBlocks* employs ET algorithm on a CBC to increase transactional speed, and at the same time, keep identities of EV secure and private. The dynamic pricing of energy consumption per unit is optimized using a non-cooperative game to maximize utility and payoffs. After maximizing profits, an event-driven time slot-based scheduling is proposed to achieve consensus on locally optimal strategies. Table 8 shows the comparative analysis of the proposed scheme against other existing approaches. The results demonstrate that the proposed scheme has higher benefits against the chosen parameters than other state-of-the-art methods.

Table 8 Comparative analysis with existing schemes

Parameters	Liang et al. [32]	Aujla et al. [5]	Mondal et al. [36]	Jindal et al. [24]	Proposed *EVBlocks*
A1	Y	Y	Y	Y	Y
A2	Y	Y	Y	Y	Y
A3	N	Y	N	Y	Y
A4	Y	Y	Y	N	Y
A5	N	Y	Y	Y	Y
A6	N	N	N	Y	Y
A7	N	N	N	Y	Y
A8	–	Y	Y	N	Y
A9	N	Y	Y	N	Y
A10	–	Y	N	Y	Y

A1: Energy Grids; A2: Multiple EVs; A3: Multiple CS; A4: Dynamic Price A5: EV utility; A6: Distributed Consensus; A7: Edge Service; A8: Event-Driven approach; A9: Game Theory; A10: Price indexing; Y: shows parameter is present; N: shows parameter is absent; & – shows parameter is not considered

6 Limitations of BC-Based ET and Possible Future Directions

In ET-based ecosystems, deploying CBC offers significant advantages of secured transaction access among authorized stakeholders. However, there are inherent challenges in securing ET through an effective network and spectrum management in V2X scenarios. By 2030, it is envisioned that massive internet-of-things (mIoT) devices would communicate, which significantly raises the processing and computing capabilities of the edge nodes. Thus, with massive and dense connectivity, there are technical and deployment challenges to integrating BC-based ET scenarios in V2X ecosystems. Some of the key challenges and potential solutions are listed as follows.

- *Computational bottlenecks in 5G-V2X and transition towards 6G*: Each CBC node is required to maintain and store a copy of the indexed ET transactional ledger, and with the rise of mIoT nodes, future V2X would require massive connection device density at the edge [52]. Although SDN addresses the network management issues through a virtualized set of services, current edge systems are required to run a local set of transactional data, which increases a significant burden in terms of storage and computation costs. Moreover, mIoT requires computations to be resource-constrained, and thus the effective realization of BC-based integration with mIoT requires lightweight consensus formation. Thus, current 5G-based v2X ecosystems face computational bottlenecks with increased participation of mIoT nodes for ET with CS through edge-based services. To increase the computational capabilities, sixth-generation (6G) is a viable fit that integrates with BC as part of its underlying protocol stack. Also, 6G allows an intelligent mix of virtualized network management through SDN and artificial intelligence-based responsive edge that can handle the vehicle mobility and dense sensor integrations [54].
- *Limitations of BC scalability*: As the number of ET transactions among EVs and CS increases, the scalability and performance of the BC networks significantly degrade.

Each node has to maintain a replica of transaction ledgers, and it directly affects the node throughput. Thus, with heavy transactional volumes in V2X, future networks are required to arbitrate effective strategies that address the limitations of transactional throughput. One possible solution is through off-chain storage, like in the case of inter-planetary file systems (IPFS), that allows data to be stored in distributed file-systems that can be accessed via authorization schemes by verified stakeholders [42]. An external reference of the file location is stored in BC through an effective hashmap structure and maintained as node replicas. Thus, each block stores more transactions, which improves the transactional throughput.

– *Resource offloading*: BC nodes are required to execute consensus algorithms, and to support mission-critical V2X communications, the bulk of the processing is shifted towards edge nodes. At present, a lot of bandwidth is required to run consensus schemes like PoW and PoS. As a possible solution, we can implement lightweight consensus schemes for support. On the other hand, we require edge-based services to provide resources to miner nodes to support the consensus formation. Thus, the underlying networks should be designed to support resilient resource offloading to edge nodes to satisfy the resource requirements [56].
– *Vulnerability of SC executions*: In BC, SC facilitates automated payments among energy stakeholders based on a defined set of logic. However, SC execution containers are vulnerable to a range of attacks like- code reentrancy, injection flaws, gas attacks, and many more that allows an adversary to divert a large number of cryptocurrency coins to their wallets. Thus, with the increase in SC execution attacks, formal SC verification is required before contract deployment for secure information exchange among transactional flows and attack scenarios [3]. Currently, a set of standards and policies for monitoring of contract environment are not standardized, and only proprietary solutions exist.
– *Involvement of third parties*: To induce trust, energy stakeholders often communicate with a trusted third-party certification authority to facilitate the trading process between EV and CS. This brings in the concept of centralization in BC, and ET requires inherent exchange through the third party. Thus, the privacy of energy stakeholders is at risk. One possible solution is combining anonymity with certificate schemes, where the public keys of stakeholders are anonymous, and thus allows privacy-preservation of ET stakeholders [6].
– *Loss of energy during ET*: In V2X, peer EVs exchange energy with each other. The transferred energy from one EV to other involves mainly a wire-based transfer. In SG communication, the power transmission line is used that suffers from heavy transmission losses. Currently, the area is an open area of research and requires effective control messages that can minimize the energy losses [53].

7 Conclusions

This paper proposed a scheme 5G-envisioned ET scheme named*EVBlocks* that integrates CBC and edge-based services in V2X environments. Through 5G location services, and based on EVs predicted distance, transactions are offloaded closer to edge nodes, thereby reducing the SDN controller latency and improving the speed of mining transactions in the blockchain. The transactional costs of EVs are then optimized by proposing a non-cooperative game that increases the profit margins of players (EVs and CSs) and eventually converges to a unique nash equilibrium state. To dampen energy fluctuations in load transfer between EVs, CS, and GS, a serial event-driven consensus termed as *PoG* is proposed that accelerates transactions through optimal local states. The limitations of the scheme are the overall complexity due to a large number of discrete parameters. This increases operational complexity, which is a critical issue. The above can be addressed in the future by reducing parameters generated during load initialization at the same desired operational efficiency.

Funding No funding available for this manuscript

Declarations

Conflicts of interest The authors declare that they have no conflict of interest statement.

References

1. Coco framework whitepaper. https://github.com/Azure/coco-framework. Accessed: (2021)-04-21.
2. Abdella, J., Tari, Z., Anwar, A., Mahmood, A., & Han, F. (2021). An architecture and performance evaluation of blockchain-based peer-to-peer energy trading. IEEE Transactions on Smart Grid pp. 1. https://doi.org/10.1109/TSG.2021.3056147.
3. Almakhour, M., Sliman, L., Samhat, A. E., & Mellouk, A. (2020). Verification of smart contracts: A survey. *Pervasive and Mobile Computing, 67,* 101227. https://doi.org/10.1016/j.pmcj.2020.101227.
4. Anand, A., de Veciana, G., & Shakkottai, S. (2020). Joint scheduling of urllc and embb traffic in 5g wireless networks. *IEEE/ACM Transactions on Networking, 28*(2), 477–490. https://doi.org/10.1109/TNET.2020.2968373.
5. Aujla, G. S., Kumar, N., Singh, M., & Zomaya, A. Y. (2019). Energy trading with dynamic pricing for electric vehicles in a smart city environment. *Journal of Parallel and Distributed Computing, 127,* 169–183.
6. Batamuliza, J., & Hanyurwimfura, D. (2020). A secure and efficient anonymous certificateless signcryption for key distribution scheme for smart grid. In: 2020 21st International Arab Conference on Information Technology (ACIT), pp. 1–7 . https://doi.org/10.1109/ACIT50332.2020.9300057.
7. Bhatia, J., Modi, Y., Tanwar, S., & Bhavsar, M. (2019). Software defined vehicular networks: A comprehensive review. *International Journal of Communication Systems, 32*(12), e4005.
8. Bhattacharya, P., Tanwar, S., Bodke, U., Tyagi, S., & Kumar, N. (2019) Bindaas: Blockchain-based deep-learning as-a-service in healthcare 4.0 applications. IEEE Transactions on Network Science and Engineering pp. 1. https://doi.org/10.1109/TNSE.2019.2961932.
9. Bhattacharya, P., Tanwar, S., Shah, R., & Ladha, A. (2020). Mobile edge computing-enabled blockchain framework—a survey. In: P.K. Singh, A.K. Kar, Y. Singh, M.H. Kolekar, S. Tanwar (eds.) Proceedings of ICRIC 2019, pp. 797–809. Springer, Cham .
10. Bodkhe, U., Bhattacharya, P., Tanwar, S., Tyagi, S., Kumar, N., & Obaidat, M.S. (2019). Blohost: Blockchain enabled smart tourism and hospitality management. In: 2019 International Conference on Computer, Information and Telecommunication Systems, Beijing, China, pp. 237–241. IEEE .
11. Bürer, M.J., de Lapparent, M., Pallotta, V., Capezzali, M., Carpita, M.: Use cases for blockchain in the energy industry opportunities of emerging business models and related risks. Computers & Industrial Engineering 137, 106002 (2019). https://doi.org/10.1016/j.cie.2019.106002. https://www.sciencedirect.com/science/article/pii/S0360835219304607
12. Chaudhary, R., Jindal, A., Aujla, G. S., Aggarwal, S., Kumar, N., & Choo, K. K. R. (2019). Best: Blockchain-based secure energy trading in sdn-enabled intelligent transportation system. *Computers & Security, 85,* 288–299.
13. Chen, S., Hu, J., Shi, Y., Zhao, L., & Li, W. (2020). A vision of c-v2x: Technologies, field testing, and challenges with chinese development. *IEEE Internet of Things Journal, 7*(5), 3872–3881. https://doi.org/10.1109/JIOT.2020.2974823.
14. Deng, R., Yang, Z., Chen, J., Asr, N. R., & Chow, M. Y. (2014). Residential energy consumption scheduling: A coupled-constraint game approach. *IEEE Transactions on Smart Grid, 5*(3), 1340–1350.

15. Do, D. T., Nguyen, T. T. T., Le, C. B., & Lee, J. W. (2020). Two-way transmission for low-latency and high-reliability 5g cellular v2x communications. *Sensors, 20*(2), 386.
16. Florea, B. C., & Taralunga, D. D. (2020). Blockchain iot for smart electric vehicles battery management. *Sustainability*. https://doi.org/10.3390/su12103984.
17. Hathaliya, J. J., Tanwar, S., Tyagi, S., & Kumar, N. (2019). Securing electronics healthcare records in healthcare 4.0 : A biometric-based approach. *Computers & Electrical Engineering, 76,* 398–410.
18. Hayes, B., Thakur, S., & Breslin, J. (2020). Co-simulation of electricity distribution networks and peer to peer energy trading platforms. *International Journal of Electrical Power & Energy Systems, 115,* 1–10. https://doi.org/10.1016/j.ijepes.2019.105419.
19. Hemadeh, I. A., Satyanarayana, K., El-Hajjar, M., & Hanzo, L. (2018). Millimeter-wave communications: Physical channel models, design considerations, antenna constructions, and link-budget. *IEEE Communications Surveys Tutorials, 20*(2), 870–913. https://doi.org/10.1109/COMST.2017.2783541.
20. Heydari, S., Fajri, P., Sabzehgar, R., & Asrari, A. (2020). Optimal brake allocation in electric vehicles for maximizing energy harvesting during braking. *IEEE Transactions on Energy Conversion, 35*(4), 1806–1814. https://doi.org/10.1109/TEC.2020.2994520.
21. Hua, S., Zhou, E., Pi, B., Sun, J., Nomura, Y., & Kurihara, H. (2018). Apply blockchain technology to electric vehicle battery refueling. In: Proceedings of the 51st Hawaii International Conference on System Sciences.
22. Jalil Piran, M., Tran, N. H., Suh, D. Y., Song, J. B., Hong, C. S., & Han, Z. (2017). Qoe-driven channel allocation and handoff management for seamless multimedia in cognitive 5g cellular networks. *IEEE Transactions on Vehicular Technology, 66*(7), 6569–6585. https://doi.org/10.1109/TVT.2016.2629507.
23. Jamil, F., Iqbal, N., Ahmad, S., & Kim, D. (2021). Peer-to-peer energy trading mechanism based on blockchain and machine learning for sustainable electrical power supply in smart grid. *IEEE Access, 9,* 39193–39217. https://doi.org/10.1109/ACCESS.2021.3060457.
24. Jindal, A., Aujla, G. S., & Kumar, N. (2019). Survivor: A blockchain based edge-as-a-service framework for secure energy trading in sdn-enabled vehicle-to-grid environment. *Computer Networks, 153,* 36–48.
25. Kabra, N., Bhattacharya, P., Tanwar, S., & Tyagi, S. (2020). Mudrachain: Blockchain-based framework for automated cheque clearance in financial institutions. *Future Generation Computer Systems, 120,* 574–587.
26. Khan Tayyaba, S., Khattak, H. A., Almogren, A., Shah, M. A., Ud Din, I., Alkhalifa, I., & Guizani, M. (2020). 5g vehicular network resource management for improving radio access through machine learning. *IEEE Access, 8,* 6792–6800. https://doi.org/10.1109/ACCESS.2020.2964697.
27. Kim, Y. M., Jung, D., Chang, Y., & Choi, D. H. (2019). Intelligent micro energy grid in 5g era: Platforms, business cases, testbeds, and next generation applications. *Electronics, 8*(4), 468.
28. Kumar, R. (2019). Report of Electric Vehicle Market-Global Opportunity analysis and Industry Forecast, 2018-2025. https://www.alliedmarketresearch.com/electric-vehicle-market (2019). [Online; accessed 26-Aug-2020].
29. Kumari, A., Gupta, R., Tanwar, S., & Kumar, N. (2020). A taxonomy of blockchain-enabled softwarization for secure uav network. *Computer Communications, 161,* 304–323. https://doi.org/10.1016/j.comcom.2020.07.042.
30. Kumari, A., Shukla, A., Gupta, R., Tanwar, S., Tyagi, S., & Kumar, N. (2020). Et-deal: A p2p smart contract-based secure energy trading scheme for smart grid systems. In: IEEE INFOCOM 2020 - IEEE Conference on Computer Communications Workshops (INFOCOM WKSHPS), pp. 1051–1056 .
31. Lee, Z.J., Li, T., & Low, S.H. (2019). Acn-data: Analysis and applications of an open ev charging dataset. In: Proceedings of the Tenth ACM International Conference on Future Energy Systems, e-Energy '19, p. 139–149. Association for Computing Machinery, New York, NY, USA (2019). https://doi.org/10.1145/3307772.3328313.
32. Liang, Y., & Zhang, X. (2018). Battery swap pricing and charging strategy for electric taxis in china. *Energy, 147,* 561–577.
33. Lin, X., Wu, J., Bashir, A. K., Li, J., Yang, W., & Piran, J. (2020). Blockchain-based incentive energy-knowledge trading in iot: Joint power transfer and ai design. *IEEE Internet of Things Journal*. https://doi.org/10.1109/JIOT.2020.3024246.
34. Liu, C., Chai, K.K., Zhang, X., & Chen, Y. (2019). Proof-of-benefit: A blockchain-enabled ev charging scheme. In: 2019 IEEE 89th Vehicular Technology Conference (VTC2019-Spring), Kuala-Lumpur, Malaysia, pp. 1–6. IEEE .
35. Meredith, J.M. (2020). 3gpp tr 22.186, service requirements for enhanced v2x scenarios. https://portal.3gpp.org/desktopmodules/Specifications/SpecificationDetails.aspx?specificationId=3180. Accessed: 2020.

36. Mondal, A., & Misra, S. (2015). Game-theoretic energy trading network topology control for electric vehicles in mobile smart grid. *IET Networks, 4*(4), 220–228.
37. Odelu, V., Das, A. K., Wazid, M., & Conti, M. (2018). Provably secure authenticated key agreement scheme for smart grid. *IEEE Transactions on Smart Grid, 9*(3), 1900–1910.
38. Rasheed, I., Hu, F., Hong, Y., & Balasubramanian, B. (2020). Intelligent vehicle network routing with adaptive 3d beam alignment for mmwave 5g-based v2x communications. *IEEE Transactions on Intelligent Transportation Systems*. https://doi.org/10.1109/TITS.2020.2973859.
39. Rosen, J. B. "Existence and Uniqueness of Equilibrium Points for Concave N-Person Games." Econometrica, vol. 33, no. 3, 1965, pp. 520–534. JSTOR, https://doi.org/10.2307/1911749. Accessed 10 July 2021.
40. Samuel, O., & Javaid, N. (2021). A secure blockchain-based demurrage mechanism for energy trading in smart communities. *International Journal of Energy Research, 45*(1), 297–315.
41. Sharma, V., You, I., & Guizani, N. (2020). Security of 5g–v2x: Technologies, standardization, and research directions. *IEEE Network, 34*(5), 306–314. https://doi.org/10.1109/MNET.001.1900662.
42. Shukla, A., Bhattacharya, P., Tanwar, S., Kumar, N., & Guizani, M. (2020). Dwara: A deep learning-based dynamic toll pricing scheme for intelligent transportation systems. *IEEE Transactions on Vehicular Technology, 69*(11), 12510–12520. https://doi.org/10.1109/TVT.2020.3022168.
43. Singh, M., & Kim, S. (2018). Branch based blockchain technology in intelligent vehicle. *Computer Networks, 145,* 219–231.
44. Soliman, H. M., & Leon-Garcia, A. (2014). Game-theoretic demand-side management with storage devices for the future smart grid. *IEEE Transactions on Smart Grid, 5*(3), 1475–1485.
45. Srinivas, J., Das, A. K., Kumar, N., & Rodrigues, J. J. P. C. (2020). Cloud centric authentication for wearable healthcare monitoring system. *IEEE Transactions on Dependable and Secure Computing, 17*(5), 942–956. https://doi.org/10.1109/TDSC.2018.2828306.
46. Srivastava, A., Bhattacharya, P., Singh, A., Mathur, A., Prakash, O., & Pradhan, R. (2018). A distributed credit transfer educational framework based on blockchain. In: 2018 Second International Conference on Advances in Computing, Control and Communication Technology (IAC3T), Allahabad, India, pp. 54–59. IEEE.
47. Su, Z., Wang, Y., Xu, Q., Fei, M., Tian, Y. C., & Zhang, N. (2019). A secure charging scheme for electric vehicles with smart communities in energy blockchain. *IEEE Internet of Things Journal, 6*(3), 4601–4613.
48. Tanwar, S., Popat, A., Bhattacharya, P., Gupta, R., & Kumar, N. A taxonomy of energy optimization techniques for smart cities: Architecture and future directions. Expert Systems **n/a**(n/a), e12703. https://doi.org/10.1111/exsy.12703.
49. Tanwar, S., Tyagi, S., & Kumar, N. (2019). *Multimedia Big Data Computing for IoT Applications: Concepts*. Paradigms and Solutions: Springer.
50. Tanwar, S., Vora, J., Tyagi, S., Kumar, N., & Obaidat, M. S. (2018). A systematic review on security issues in vehicular ad hoc network. *Security and Privacy, 1*(5), e39. https://doi.org/10.1002/spy2.39.
51. Tedeschi, P., Piro, G., Murillo, J. A. S., Ignjatov, N., Pilc, M., Lebloch, K., & Boggia, G. (2019). Blockchain as a service: Securing bartering functionalities in the h2020 symbiote framework. *Internet Technology Letters, 2*(1), e72. https://doi.org/10.1002/itl2.72.
52. Wang, K., Chen, C. M., Liang, Z., Hassan, M. M., Sarné, G. M., Fotia, L., & Fortino, G. (2021). A trusted consensus fusion scheme for decentralized collaborated learning in massive iot domain. *Information Fusion, 72,* 100–109. https://doi.org/10.1016/j.inffus.2021.02.011.
53. Wang, K., Wang, W., Wang, L., & Li, L. (2020). An improved soc control strategy for electric vehicle hybrid energy storage systems. *Energies*. https://doi.org/10.3390/en13205297.
54. Xu, H., Klaine, P. V., Onireti, O., Cao, B., Imran, M., & Zhang, L. (2020). Blockchain-enabled resource management and sharing for 6g communications. *Digital Communications and Networks, 6*(3), 261–269. https://doi.org/10.1016/j.dcan.2020.06.002.
55. Yun, J., Piran, M. J., & Suh, D. Y. (2018). Qoe-driven resource allocation for live video streaming over d2d-underlaid 5g cellular networks. *IEEE Access, 6,* 72563–72580. https://doi.org/10.1109/ACCESS.2018.2882441.
56. Zhang, H., Wang, Z., & Liu, K. (2020). V2x offloading and resource allocation in sdn-assisted mec-based vehicular networks. *China Communications, 17*(5), 266–283.
57. Zhang, T., Pota, H., Chu, C. C., & Gadh, R. (2018). Real-time renewable energy incentive system for electric vehicles using prioritization and cryptocurrency. *Applied Energy, 226,* 582–594.

Pronaya Bhattacharya is employed as an Assistant Professor in Computer Science and Engineering Department at the Institute of Technology, Nirma University, Ahmedabad, Gujarat, India. He has more than 8 years of teaching experience. He has completed PhD in Optical Networks from Dr. A. P. J Abdul Kalam Technical University, Lucknow, Uttar Pradesh, India. He has authored or co-authored 40 research papers in leading SCI journals and top A* core IEEE ComSoc conferences. Some of his top findings are published in IEEE-TVT, IEEE-TNSE, John Wiley- ETT, Elsevier- FGCS, Kuwait University- JER, IEEE-InfoCom, IEEE-ICC and IEEE-CITS. He is working as a reviewer of reputed SCI journals- IEEE-TII, IEEE Network, IEEE-Access, John Wiley-ETT, John-Wiley-SPS, John Wiley- IJCS, Elsevier-OSN, and Kuwait University-JER. He is awarded the best paper award in Springer ICRIC-2019. He has also been appointed as Session Chair in the IC4S-2019, IC4S-2020, IICT-2020, and PDGC-2020. His research interests include optical switching, high performance networking, blockchain, IoT and deep learning. He is a lifetime member of professional societies like ISTE and IAENG.

Sudeep Tanwar (M'15, SM'21) is a Full Professor in the Computer Science and Engineering Department at the Institute of Technology, Nirma University, Ahmedabad, Gujarat, India. He is a visiting Professor at Jan Wyzykowski University in Polkowice, Poland, and at the University of Pitesti in Pitesti, Romania. He received a B.Tech. in 2002 from Kurukshetra University, India, an M.Tech (Honors) in 2009 from Guru Gobind Singh Indraprastha University, Delhi, India, and a PhD in 2016 with specialization in Wireless Sensor Networks. He has authored or coauthored more than 200 technical research papers published in leading journals and conferences, such as IEEE TRANSACTIONS ON NETWORK SCIENCE AND ENGINEERING, IEEE TRANSACTIONS ON VEHICULAR TECHNOLOGY, IEEE TRANSACTIONS ON INDUSTRIAL INFORMATICS, IEEE WIRELESS COMMUNICATIONS, IEEE NETWORKS, ICC, GLOBECOM, and INFOCOMtop journals and top conferences, such as IEEE TRANSACTIONS ON NETWORK SCIENCE AND ENGINEERING, IEEE TRANSACTIONS ON VEHICULAR TECHNOLOGY, IEEE TRANSACTIONS ON INDUSTRIAL INFORMATICS, IEEE WIRELESS COMMUNICATIONS, IEEE NETWORKS, ICC, GLOBECOM, and INFOCOM. He has edited/authored books with International/National Publishers like IET and Springer. He has guided many students to M.Eng./M.Tech. degrees, and has guided students to a PhD. He is an Associate Editor of IJCS (Wiley) and Security and Privacy Journal (Wiley). His current interests include Wireless Sensor Networks, Fog Computing, Smart Grids, the IoT, and Blockchain Technology. He has received best research paper awards from ECAI-2021, IEEE IWCMC-2021,IEEE GLOBECOM 2018, IEEE ICC 2019, and Springer ICRIC-2019. He is also leading the ST Research Laboratory, where group members are working on the latest cutting-edge technologies.

Umesh Bodkhe is currently pursuing a Ph.D. degree with Nirma University, Ahmedabad, India. He is currently working as an Assistant Professor in computer science and engineering with the Department at Institute of Technology, Nirma University. His current research interests include network security, IoT,6G, and blockchain technology. He is a Lifetime Member of the ISTE. He has published more than 15 research papers in leading SCI/Scopus/WoS journals- IEEE- Access, John Wiley- ETT, IEEE-TNSE, John Wiley- SPE, IET Software journal, and conferences- IEEE- CITS-2019, Springer- IC4S-2019. He is working as a reviewer of reputed SCI/Scopus journals- IEEE- Access, Elsevier- IJIM, , and John Wiley-ETT.

Ashwani Kumar is currently working as an Associate Professor in the Department of Computer Science and Engineering at Vardhaman College of Engineering, (AUTONOMOUS) Hyderabad, Telangana, India. He received his doctorate of philosophy (Ph.D) in Computer Science and Engineering, from Jaypee University of Information Technology, H.P in 2017. He received his M.Tech (CSE) from Jaypee University of Information Technology, H.P in 2011. He has done B.Tech from Uttar Pradesh Technical University (U.P.T.U) Lucknow, U.P in 2009. He has more than 9 years of teaching and research experience. He published more than 25 research papers in international reputed journals indexed in Web of Science & SCOPUS and top rank conferences as authored or co-authored. His research findings are published in Procedia Computer Science Elsevier, JST Universiti Putra Malaysia, IJCAC IGI Global USA, IEEE Xplore. He is serving as the reviewer of many SCI Journals- IET Information IET Digital Library, Multimedia Tools and Application (MATP) Springer, National Academy Science Letters Springer, Journal of Intelligent and Fuzzy Systems (JIFS) IOS Press. Currently, he is editorial board member of many reputed Journals-IJDCF, IJISP, IJEUCD, IGI Global Journal USA indexed in WoS/Scopus. He has been guest editor for International Journal Recent Patent of Engineering, Bentham Publication indexed in SCOPUS. He is the Book Series Editor of : Advancements in Security and Privacy Initiatives for Multimedia Images, IGI Global Journal USA. He is awarded as Bentham Brand Ambassador Award for the year 2019-2020. He served as session chair in several international conferences-ICIIP-2019, MISS-2020, IC4S-2020, PGDC-2020. He has filing an Australian patent in the year 2020. His research area includes Image Security, Watermarking Techniques, Multimedia Application, Security & Privacy, Cryptography and Network Security. He is also a lifetime member of professional societies like ISTE, IACSIT, IAENG and SDIWC.

Neeraj Kumar (M'16, SM'18) received his PhD in CSE from Shri Mata Vaishno Devi University, Katra (J&K), India. He was a postdoctoral research fellow at Coventry University, Coventry, UK. He is currently a Full Professor in the Department of Computer Science and Engineering, Thapar University, Patiala (Pb.), India. He has published more than 400 technical research papers in leading journals and conferences from IEEE, Elsevier, Springer, John Wiley, etc. Some of his research findings were published in top-cited journals such as IEEE TIE, IEEE TDSC, IEEE TITS, IEEE TCC, IEEE TKDE, IEEE TVT, IEEE TCE, IEEE Netw., IEEE Comm., IEEE WC, IEEE IoTJ, IEEE SJ, FGCS, JNCA, and ComCom. He has guided many PhD and M.Eng./M.Tech. students. His research was supported with funding from Tata Consultancy Service, the Council of Scientific and Industrial Research (CSIR), and the Department of Science & Technology. He received best research paper awards from IEEE ICC 2018 and IEEE Systems Journal 2018. He is leading the research group Sustainable Practices for Internet of Energy and Security (SPINES), where group members are working on the latest cutting-edge technologies. He is a TPC member, and a reviewer for many international conferences across the globe. He is a visiting professor at Coventry University, Coventry, UK, and a senior member of IEEE.

Authors and Affiliations

Pronaya Bhattacharya[1] · Sudeep Tanwar[1] · Umesh Bodkhe[1] · Ashwani Kumar[2] · Neeraj Kumar[3,4,5]

Pronaya Bhattacharya
pronoya.bhattacharya@nirmauni.ac.in

Umesh Bodkhe
umesh.bodkhe@nirmauni.ac.in

Ashwani Kumar
ashwani.kumarcse@gmail.com

Neeraj Kumar
neeraj.kumar@thapar.edu

1 Department of Computer Science and Engineering, Institute of Technology, Nirma University, Ahmedabad, Gujarat, India

2 Sreyas Institute of Engineering and Technology, Nagole, Hyderabad, India

3 Thapar Institute of Engineering and Technology, Deemed to be University, Patiala, Punjab, India

4 The University of Petroleum and Energy Studies, Dehradhun, India

5 Department of Computer Science and Information Engineering, Asia University, Taiwan, Taiwan